Graduation Design (Thesis) of Chongqing University

# Green Energy Island Integration and Operation Optimization Research


**Undergraduate Student: Jie Xu**

**Student Number: 20143503**

**Supervisor: Prof. Chen Yang**

**Major: Sustainable Energy Science and Engineering**

**College of Power Engineering**

**Chongqing University**


**June, 2018**

重庆大学本科学生毕业设计（论文）

# 绿色能源岛集成与优化运行研究

学　　生：许 杰

学　　号：20143503

指导教师：杨 晨

专　　业：新能源科学与工程

重庆大学动力工程学院

2018 年 6 月

# 摘　　要

传统的集中式电网逐渐地成为了现代能源系统的不稳定因素，因为它们效率低，脆弱，适应性差。人们逐渐意识到只有通过多种能源供给，电网去中心化以及正确匹配能量和热机才能解决以上问题。分布式能源系统效率高，适应性强，抗灾害能力强，并且能够促进当地经济发展和社会进步。但是，要设计和管理它们相对来说更复杂。现在世界各地在展开越来越多的研究来加速它们的应用。优化是设计分布式能源系统最有效的方法之一，因为分布式能源系统的参数可达几千个，种类也很多，仅仅使用现存的热力设计工程手册是不能完成整个项目设计的，建模、分析和优化正在逐渐代替过去的依靠手册进行查阅和计算的旧模式。

绿色能源岛实验教学平台由重庆大学动力工程学院搭建，这个项目的对象是基于绿色能源岛的简化版分布式能源系统，忽略带有动态特性的设备之后，这个系统主要由微型燃气轮机、吸收式制冷机、有机朗肯发电机、热泵、蒸汽压缩制冷机以及其他可再生发电设备组成，并且和外界电网相连，同时产生电力、饱和热蒸汽和冷水三种产品。通过燃烧天然气，微型燃气轮机产生电和蒸汽，其排出的尾气驱动吸收式制冷机和有机朗肯发电机，热泵和蒸汽压缩制冷机是电驱动。其他可再生发电设备利用阳光和风资源。

在这个项目中，假设整个系统运行在额定工况，这就意味着每个循环都是准静态平衡过程，然后据此编写几个静态模型。首先进行预分析，然后使用遗传算法来优化整个系统。根据预分析的结果创造出组成的初始种群之后，通过限制可行区间，利用选择、交叉和突变三种操作在上一代的基础上产生下一代种群。每代种群的每个个体都通过适应性函数计算来得到适应值，这可以表明这个组合是否适合被用来设计该系统，基于适应值的选择过程会确保每代种群的设计参数组合的数量是不变的。

上文提到的预分析是为了确定空气-烟气比和热电比（冷电比）。假设热蒸汽和冷水之间有一个是主要产品，比如说，案例分析中的位于中国南方的绿色能源岛总体上要提供更多的冷水，所以要把微型燃气轮机的出口烟气温度设得相对比较高，计算冷电比以优先满足冷负荷。所有的辅助参数确定好之后，整个系统的优化才能进行，这样可以大大减少优化所需要的时间。

在编写数学模型的时候，不同工质的热力性质计算和㶲分析是两个最重要的操作。这个项目探究了五个热力参数即温度、压力、比体积、焓和熵之间的比较重要的相互关系，这些关系确保了模型结果的准确性和实用性。此外，所有的设备每个

组件都以㶲损和㶲效率的方式进行了分析，以显示其真正的热力学性能。

然而，有一些问题是不能忽视的，这需要进一步地探究。因为缺少实际参数、扎实的工程经济知识和丰富的相关经验，热经济学分析不得不放弃，适应性函数中的经济因素的缺失导致优化结果偏离。此外，因为各种工质的焓和熵的计算需要统一，而且通过压力和熵来计算温度实在是太难了，所以项目中的某些计算是通过调用一个非原创程序来完成的。

尽管遇到了各种各样的困难，但是项目的结果还是非常振奋人心的。评估失败频率的下降和适应值的提高证明了这个项目的大多数思想的正确性，另外也产生了很多的辅助结果，这对更好地理解整个分布式能源系统有很大帮助。总而言之，这个项目较困难，完成得较好，也需要进一步的研究。

# 关键字

分布式能源系统，系统集成，最优化，遗传算法，㶲分析

# Abstract

Traditional centralized electricity grid is gradually becoming a destabilizing factor in modern energy system, because of its low efficiency, vulnerability and poor flexibility. People come to realize that only by providing more kinds of energy, decentralizing electricity gird and matching heat with corresponding heat engine can energy system solve above problems. Distributed Energy Resources (DER) Systems are efficient and adaptable, easy to deploy, able to resist natural disasters. Moreover, they harness local economic and social development. However, they are relatively more complex to design and manage. Nowadays, lots of researches across the world have been performed to accelerate the application of DER systems. Optimization is one of the most effective ways to design a DER systems. With number of variables in DER systems reaching thousands and various kinds of DER systems, existing engineering handbook for thermal design can no longer be used alone to finish the whole design process. Modeling, analysis and optimization is replacing past reading and calculating according to handbooks.

Green Energy Island platform for experiment and instruction has been established by Power Engineering College of Chongqing University. This project is carried out to perform optimization of a simplified DER system based on Green Energy Island. It is grid-connected and composed of a micro gas turbine, an absorption chiller, an organic rankine turbine, a heat pump, a vapor compression chiller and some renewable electricity generators, while other devices with dynamic characteristics are neglected. This DER system produces electricity, saturated hot steam, and cold water at the same time. Micro gas turbine provides electricity and steam by combusting natural gas. The absorption chiller and organic rankine turbine are heat-driven by the waste gas from micro gas turbine, while the heat pump, and vapor compression chiller are electricity-driven. Other renewable electricity generators utilize sun light or wind.

In this project, it's assumed that the whole system operates in rated condition, which means every cycle is quasi-equilibrium process. And several static thermal mathematical models are constructed. Some pre-analyses are performed at first. Then, genetic algorithm is employed to optimize the whole system. The initial population of variable combination is created according to pre-analyses. By restricting within feasible region, then comes next generations, which is generated by selection, crossover and mutation based on the

previous generation. Each individual in every generation is evaluated by fitness function and get a fitness value showing whether it's appropriate to be adopted to design the DER system. Based on the fitness value, the process of selection makes sure the number of individuals in each generation is the same.

Pre-analyses mentioned above is to determine the air-gas ration and heat-power/cold-power ratio. It's assumed that there is a major product between hot steam and cold water. For example, the case study has chosen the green energy island in southern China, which means more cold water must be supplied than hot steam in general. So, the outlet temperature of waste gas of micro gas turbine is set relatively high and cold-electricity ratio is calculated to meet load of cold water in priority. Whole optimization must be carried out after all assisting variables are determined, because these analyses can shorten the time of optimization enormously.

When constructing mathematical model, the calculation for thermal properties of different working substances and the exergy analysis are two most important operation. Some important interactions between five thermal properties, temperature, pressure, specific volume, enthalpy and entropy, are explored in this project. It's these relationships that make the result of model accurate and practical. Additionally, each component in every device has been analyzed in the form of exergy destruction and efficiency, which indicate the actual thermodynamic performance.

However, some problems cannot be neglected, and they need further attention. Thermo-economics analysis has to be abandoned for lack of collected actual parameters, solid engineering economics knowledge and rich related experience. So, the economic factors in fitness are missing, resulting in deviation of optimization. Besides, the calculations for enthalpy and entropy of various working substances need unification, and it's hard to compute temperature based on pressure and entropy. So, some of the calculation in this project is done by calling non-original program.

In spite of various troubles, the result of this project is rather encouraging. The decreasing frequency of evaluation failure and increasing fitness value prove most ideas in this project right. And there are lots of supplementary results achieved, which helps to understand the whole DER system. In a nut shell, this project is finished well and needs further researching.

# Key Words

Distributed Energy System, System Integration, Optimization,
Genetic Algorithm, Exergy Analysis

# Table of Content

*摘要* ..... *1*

*关键字* ..... *2*

*Abstract* ..... *3*

*Key Words* ..... *5*

*Chapter 1 Introduction* ..... *9*

1.1 Research Background ..... 9

1.2 Review of Previous Research ..... 10

1.3 Basic Structure of this System ..... 11

*Chapter 2 Thermal System Modeling* ..... *15*

2.1 Introduction to Thermal System Modeling ..... 15

2.2 Gas Power Cycle (Brayton Gas Cycle) ..... 16

2.2.1 Gas Power Cycle and Brayton Cycle ..... 16

2.2.2 Calculation of Ma-Mg Ratio (RaAG) ..... 17

2.3 Ideal Rankine Cycle and Organic Rankine Cycle ..... 19

2.3.1 Ideal Rankine Cycle ..... 19

2.3.2 Organic Rankine Cycle ..... 20

2.4 Refrigeration Cycle ..... 21

2.4.1 Ideal Vapor Compression Refrigeration Cycle ..... 21

2.4.2 Ideal Absorption Refrigeration Cycle ..... 22

2.4.3 Absorption Refrigeration Cycle & Vapor Compression Refrigeration Cycle ..... 24

2.5 Ideal Heat Pump Cycle ..... 25

*Chapter 3 Integration of Thermal Systems* ..... *27*

3.1 Exergy Analysis of Thermal Systems ..... 27

3.1.1 Exergy Equation ..... 27

3.1.2 Physical Exergy ..... 28

3.1.3 Chemical Exergy ..... 28

3.1.4 Exergy Efficiency ..... 29

3.2 Principle of Cascading Utilization ..... 32

3.3 Principle of Multi-Energy Complementation ..... 34

*Chapter 4 Optimization of DER System* ..... *39*

4.1 Introduction to Optimization ..... 39

**4.2 Optimization using Genetic Algorithm** ..... **40**
4.2.1 Introduction to Genetic Algorithm ..... 40
4.2.2 Generation, Population and Diversity ..... 41
4.2.3 Algorithms for Solving Nonlinear Constraint ..... 41
**4.3 Optimization of DER System in GEI** ..... **42**
4.3.1 Introduction to Optimization of DER System in GEI ..... 42
4.3.2 Decision Variables in Optimization of DER System in GEI ..... 44
4.3.3 Fitness Function for Optimization of DER System in GEI ..... 45
***Chapter 5 Thermal Properties of Working Substances*** ..... ***47***
**5.1 Introduction to Thermal Property** ..... **47**
**5.2 Equation of State** ..... **47**
5.2.1 Introduction to Equation of State ..... 47
5.2.2 Application of Peng-Robinson Equation of State ..... 47
**5.3 Calculation of Enthalpy and Entropy** ..... **49**
**5.4 Vapor Pressure and Liquid Density** ..... **52**
**5.5 Temp and Pressure of Binary Saturated Solution** ..... **53**
**5.5 Softwares for Thermal Property** ..... **53**
5.5.1 REFPROP ..... 53
5.5.2 CoolProp ..... 54
***Chapter 6 Case Study & Result*** ..... ***55***
**6.1 Optimization of MGT** ..... **55**
**6.2 GEI in Southern China** ..... **56**
***Chapter 7 Conclusion*** ..... ***59***
***Acknowledgements*** ..... ***61***
***Reference*** ..... ***63***

# Chapter 1 Introduction

We are facing more and more urgent energy-economy-environment problems. The past experience has indicated that the centralized energy systems are out of date in today's planet because of low-efficiency, energy waste and high-risk. Green Energy Island has been proposed to replace them, which integrates several energy technologies and are able to track the fluctuation of energy demand to save primary energy. However, only by careful design and optimization can we build the qualified Green Energy Island to improve thermodynamic and economic efficiency and avoid strict energy management in unusual conditions. The techniques from Artificial Intelligence (AI) can make a difference in this task. Through this research task, I will go over the past knowledge, become familiar with academic research, and more energetic to continue study life in energy system analysis.

There are two types of optimization of DER system, with one focusing on static processes, which is configuration optimization, and the other one being operation optimization focusing on dynamic processes. Configuration optimization can be divided into two parts, structure and parameter optimization. With more and more new ways to generate electricity like wind turbines, PV cells, ocean wave generator, etc, the energy system can be composed of various schemes and scales, which can be seen as the application of principle of multi-energy complementary. When the structure is decided according to the local geographical condition and other factors, designers have to calculate each component's parameters. After establishing detailed mathematical model of the whole system, the control strategy must be set to meet the changing demand of the local electricity and heat or cool water, which is the operation optimization. Among all these process, the choices of numbers of heat engines, capacity of each facilities, electricity and heat storage devices are the most important task.

## 1.1 Research Background

Energy is one of the essential needs of a functioning society, and concerns about the sustainability of present energy-use practices are now arising in several areas: the rapid depletion of nonrenewable resources, the impacts of emissions on the global environment, and global instabilities that affect the security of supplies. [1] One effect way to meet the challenges is to switch from the conventional centralized energy generation and long-

range energy transmission, to small-scale, inter-connected energy generation through the adoption of distributed energy resource (DER) systems, as well as energy management.

DER systems provide numerous advantages over centralized generation. First, by locating generation units closer to the consumer, transmission and distribution losses are minimized. Second, some DER technologies, like combined heating and power (CHP) and combined cooling, heating and power (CCHP) can recycle waste energy to generate additional usable energy streams thus increasing the thermodynamic efficiency and minimizing the primary energy consumption. Additionally, DER systems allow for the utilization of local renewable resources (e.g. indigenous biomass sources), and add a degree of flexibility, resilience, and control to the way in which energy is provided to the consumer. [2] [3] [4] However, unlike the large of amount of electricity supply of centralized generation, DER systems rely on the consistency between supply and demand, which stresses the importance of proper design and optimization.

It can be relatively easy to design a traditional thermal power station, since there are a lot of design handbooks and recommended data and cases. And the structure of those system is more invariable and less complicated. Also, because of their weakness in load tracking, those systems are not designed to operate in variable working condition. In contrast, there are many different components in DER systems, which have complex connections between each other. And they have to be carefully tailored to local conditions. Moreover, operation strategies have to examined in various operating conditions to meet different demand. All these factors have made designing DER systems a hot potato. However, as the development of computer-aided design and optimization methods, DER systems are becoming more and more widely used.

## 1.2 Review of Previous Research

There is a number of studies analyzing energy tools. To name a few, Cormio et al.v discussed the EFOM energy tool, Faraji-Zonooz et al.vi provided a complete review of the MARKAL energy tool, Ball et al. [5] demonstrated the MOREHyS energy tool (which is based on the BALMOREL tool), Tsioliaridou et al. [6] assessed the Invert energy tool and finally, Cai et al. [7] discussed the UREM energy tool. Lambert et al. [8] provided a detailed description of modeling using HORMER, which had been developed by National Renewable Energy Laboratory in the USA.

In addition to various compiled computer tools, there are many ways to formulate the distributed energy planning problem, like using the mixed integer linear programming

framework. Some studies deal with operation optimization of the system mainly with single technology or fuel. For example, Chinese and Meneghetti (2005) [9] developed optimization models for the design of biomass-based district heating networks for an industrial district with an aim to maximize the utility company's profit and also to minimize greenhouse gas emissions. However, the majority of studies deal with optimal technology selection and unit dispatch with a wider set of technologies. [10] [11] [12] [13] Dicorato et al. (2008) [14] created an energy flow optimization model for the integration of distributed generation into a regional energy system. The objective function was the minimization of the energy production cost, and the model employed a multi-period linear approach. Angrisani et al. (2012) [15] analyzed the energy, economic, and environmental performance of micro tri-generation systems. Hawkes and Leach (2009) [16] increased the complexity further by constructing a unit dispatch model for a micro grid with the inclusion of electricity and thermal storage.

## 1.3 Basic Structure of this System

The object is a grid-connected distributed energy system, called **Green Energy Island (GEI)**, composed of a variety of energy technologies. It satisfies the need of people and equipments in a remote island by supplying electricity, hot steam, and cooling. There are three facilities, **Micro Gas Turbine (MGT)**, **Aqueous Lithium-Bromine Single-Effect Absorption Chiller (AC_ALB)**, and **R123 Organic Recycle Cycle (ORC_R123)**, providing the majority of three products. Nature gas or other substituted fuel burns in MGT to produce electricity, with waste heat recovered by AC_ALB and ORC_R134a. One produces cool water, and the other one produces electricity. There is also energy from the sun collected through **Photovoltaic Modules (PV)** and **Concentrating Solar Thermal Collector (CST)**. PV can produce electricity, and CST can produce hot steam. Electricity can also be generated by **Wind Turbine (WT)**. Besides, if the load of hot steam and cooling cann't be met, **Heat Pump (HP)** and **R134a Vapor Compression Chiller (VCC_R134a)** can be powered to supply hot steam and cooling, respectively. If the electricity generated is consumed to supply other products, it can be bought from **National Grid (NG)**. The overall illustration of the system is shown in Figure 1.1.

Every technology has its own advantage and disadvantage, but an integrated system based on many kinds of technologies get the ability of play strengths and overcome the shortcomings, which is the idea of Multi-energy Complementation. Because different

energy sources can complement each other to some extent, multi-source hybrid energy systems (with proper integration and control) have great potential to provide higher quality and more reliable power to customers than a system based on a single resource. Because of this feature, hybrid energy systems have caught worldwide research attention. [17]

The tracking response of MGT is relatively in high speed and the GER system is small enough to ignore the effect of relaxation time, so I simply the system to be a quasi-equilibrium process, which means time dimension are neglected in optimization. Otherwise, the mathematical can become so complicated that each iteration contains the process of control optimization, which can even be more time consuming that the configuration optimization process itself. On the other hand, this model can only represent the rated operating condition with no extra hot steam and cooling produced. Electricity can be sold to or bought from national grid. So, the intermittency of load in Green Energy Island and weather condition must be neglected, which restricts this model's scope of application. But I will continue related work during my master program.

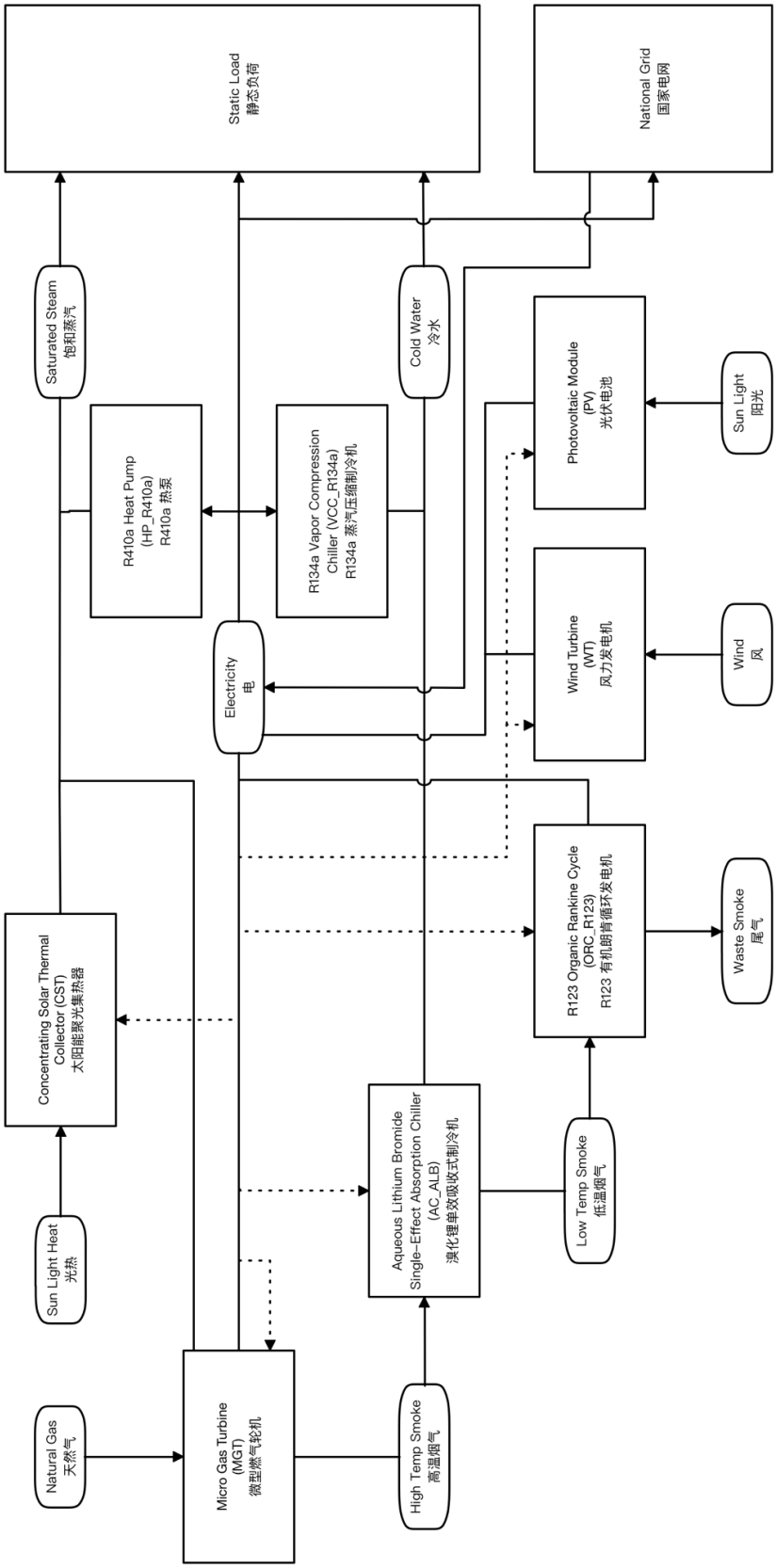


Figure 1.1 Structure illustration of Distributed Energy System in Green Energy Island

# Chapter 2 Thermal System Modeling

## 2.1 Introduction to Thermal System Modeling

The performance of the thermal system is determined by the thermal state parameters of the working fluid in the system and the structural parameters of the equipment and components that make up the system. These parameters can be divided into different values according to the way: Some parameters are independent variables determined by external contact conditions, such as residual heat inlet temperature, flow rate, ambient temperature, and atmospheric pressure; some independent variables may have values The constraint conditions constitute a free change in the feasible domain, but when the value of this part of the independent variables is determined, all other parameters of the relevant variables are uniquely determined by the physical equations of energy conservation, mass conservation, and flow pressure drop of the equipment in the system.

The independent variables of the system can be divided into independent variables of thermal parameters and independent variables of structural parameters. The number of independent variables of the thermal parameters can be obtained by assuming that the system control equations composed of various physical equations have definite solutions, assuming that the values of the independent variables of the structural parameters of all the devices in the system are determined.

The internal devices of the thermal system are related to the transfer of the flow of energy through the working fluid between the external system and the external system. The status of the general flow is required to determine the flow rate and two parameters of the thermal state (such as temperature and pressure), which are three parameters of the carrier energy. However, when one of the thermal state parameters remains unchanged, the change is small, or the effect of the change on the system performance is negligible, only two parameters are needed to determine the state of the working fluid flow, which belongs to the two-parameter carrier energy. In addition, as far as the scope and purpose of this study, such as the input of components, the output of electrical energy or mechanical energy, it is only necessary to know the number of the components and it is a single-parameter carrier energy.

## 2.2 Gas Power Cycle (Brayton Gas Cycle)

### 2.2.1 Gas Power Cycle and Brayton Cycle

Gas turbines usually operate on an open cycle, as shown in Figure 2.1. Fresh air at ambient conditions is drawn into the compressor, where its temperature and pressure are raised. The high-pressure air proceeds into the combustion chamber, where the fuel is burned at constant pressure. The resulting high-temperature gases then enter the turbine, where they expand to the atmospheric pressure while producing power. The exhaust gases leaving the turbine are thrown out (not recirculated), causing the cycle to be classified as an open cycle. The process is shown in Figure 2.1 and Figure 2.2.

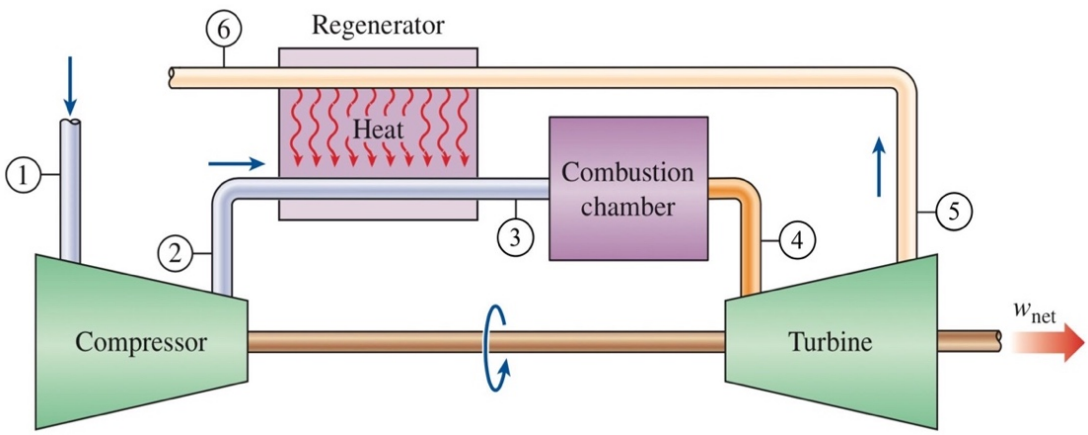


Figure 2.1 Illustration of a gas-turbine with regenerator

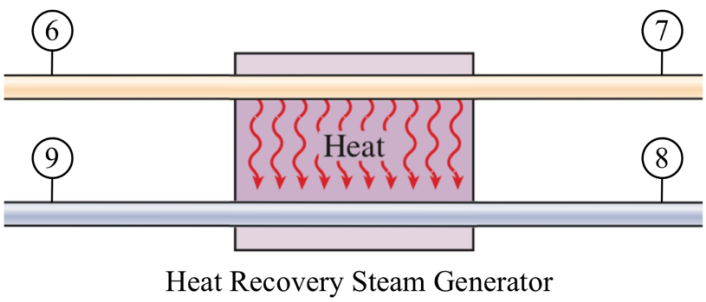


Figure 2.2 Illustration of a heat recovery steam generator

The open gas-turbine cycle described above can be modeled as a closed cycle, as shown in Figure 2.3a, by utilizing the air-standard assumptions. Here the compression and expansion processes remain the same, but the combustion process is replaced by a

constant-pressure heat-addition process from an external source, and the exhaust process is replaced by a constant-pressure heat-rejection process to the ambient air. The ideal cycle that the working fluid undergoes in this closed loop is the Brayton cycle, which is made up of four internally reversible processes:

- 1-2 Isentropic compression (in a compressor)
- 2-3 Constant-pressure heat addition
- 3-4 Isentropic expansion (in a turbine)
- 4-1 Constant-pressure heat rejection

In gas-turbine engines, the temperature of the exhaust gas leaving the turbine is often considerably higher than the temperature of the air leaving the compressor. Therefore, the high-pressure air leaving the compressor can be heated by transferring heat to it from the hot exhaust gases in a counter-flow heat exchanger, which is also known as a regenerator (MGTre).

Figure 2.3b is a T-s diagram of the gas turbine with regenerator plotted by program in this project, *Plot_GEI_MGT_Exergy*, through MATLAB. **P_2 = 637317.19**, **Eta_MGTac = 0.8988861**, **Eta_MGTt = 0.923143**, **T_3 = 699.999574**, **T_4 = 1100**.

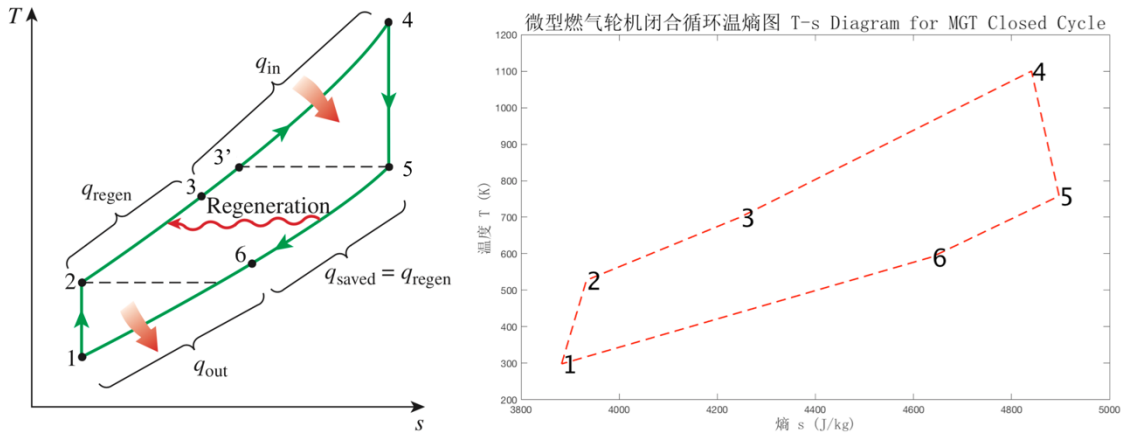


Figure 2.3a & Figure 2.3b T-S Diagram of a Gas Turbine with Regenerator

## 2.2.2 Calculation of Ma-Mg Ratio (RaAG)

The calculation of combustion process not only reveals the status change of fuel, but also allow the following heat exchange process to be calculated. And it's one of the most complicated calculation in MGT model. Firstly, elements of theoretical gas are explored by the following code.

```
% Theoratical Gas
y_O = 0.21;              % Volume fraction of Oxygen in Air.
n_aC = 2 / y_O;           % Needed air for 1 mol fuel combustion
n_gC = 1 + 2 + n_aC - 2;  % Waste gas from combustion with just needed air
y_C = (1 + n_aC * 0.0004) / n_gC;
y_H = 2 / n_gC;
y_N = 1 - y_C - y_H;
MgC = y_C * 44 + y_H * 18 + y_N * 28;
M_AC = n_aC * 29 / 16;
MgC = n_gC * MgC / 16;
```

Secondly, **RaAGsyms** is assumed as the symbol variable representing Ma-Mg Ratio (**RaAG**) in MATLAB to express the symbol variable of **Cp_g**, specific heat at constant pressure of gas after combustion. Then, solve the combustion equation and get **RaAG**. Here is the code.

```
syms Hsyms
    % Calculate the h, s, E_ph of gas in status 4.
    H_a4 = CoolProp.PropsSI('H', 'T', T_4, 'P', P_4, 'Air');
    S_a4 = CoolProp.PropsSI('S', 'T', T_4, 'P', P_4, 'Air');
    H_H4 = CoolProp.PropsSI('H', 'T', T_4, 'P', P_4, 'Water');
    S_H4 = CoolProp.PropsSI('S', 'T', T_4, 'P', P_4, 'Water');
    H_C4 = CoolProp.PropsSI('H', 'T', T_4, 'P', P_4, 'CarbonDioxide');
    S_C4 = CoolProp.PropsSI('S', 'T', T_4, 'P', P_4, 'CarbonDioxide');
    H_N4 = CoolProp.PropsSI('H', 'T', T_4, 'P', P_4, 'Nitrogen');
    S_N4 = CoolProp.PropsSI('S', 'T', T_4, 'P', P_4, 'Nitrogen');
    H_g4syms = (Hsyms - (1-Hsyms)/16*2/0.21*29) * H_a4 + ...
             ((1-Hsyms)/16*2/0.21*29) * y_H*18/MgC * H_H4 + ...
             ((1-Hsyms)/16*2/0.21*29) * y_C*44/MgC * H_C4 + ...
             ((1-Hsyms)/16*2/0.21*29) * y_N*28/MgC * H_N4;
    S_g4syms = (Hsyms - (1-Hsyms)/16*2/0.21*29) * S_a4 + ...
             ((1-Hsyms)/16*2/0.21*29) * y_H*18/MgC * S_H4 + ...
             ((1-Hsyms)/16*2/0.21*29) * y_C*44/MgC * S_C4 + ...
             ((1-Hsyms)/16*2/0.21*29) * y_N*28/MgC * S_N4;
    Cp_gsyms = (H_g4syms - H_g0syms) / (T_4 - T_0);
SHsyms = solve(Hsyms == (T_4 * Cp_gsyms - Eta_MGTcc * LHV) / ...
             (H_a3 - Eta_MGTcc * LHV));
H = double(SHsyms);
```

Finally, the flow rates of air, fuel and gas are computed by the following equation.

```
Mg = Wp_MGT / ((H_g4 - H_g5) - (H_a2 - H_a1)*H);
Ma = H * Mg;
```

```
Mf = Mg - Ma;
Ma_x = Ma - Mf/16*2/0.21*29;
```

## 2.3 Ideal Rankine Cycle and Organic Rankine Cycle

### 2.3.1 Ideal Rankine Cycle

As we all know, Carnot cycle is the most efficient cycle operating between two specified temperature limits. The fluid is heated reversibly and isothermally in a boiler (process 1-2), expanded isentropically in a turbine (process 2-3), condensed reversibly and isothermally in a condenser (process 3-4), and compressed isentropically by a compressor to the initial state (process 4-1). Carnot cycle cannot be approximated in actual devices and is not a realistic model for vapor power cycles.

Water enters the pump at status 1 as saturated liquid and is compressed isentropically to the operating pressure of the boiler. The water temperature increases somewhat during this isentropic compression process due to a slight decrease in the specific volume of water. Water enters the boiler as a compressed liquid at state 2 and leaves as a superheated vapor at state 3. The superheated vapor at state 3 enters the turbine, where it expands isentropically and produces work by rotating the shaft connected to an electric generator. The pressure and the temperature of steam drop during this process to the values at state 4, where steam enters the condenser. At this state, steam is usually a saturated liquid–vapor mixture with a high quality. Steam is condensed at constant pressure in the condenser, which is basically a large heat exchanger, by rejecting heat to a cooling medium such as a lake, a river, or the atmosphere. Steam leaves the condenser as saturated liquid and enters the pump, completing the cycle. The process is shown in Figure 2.4.

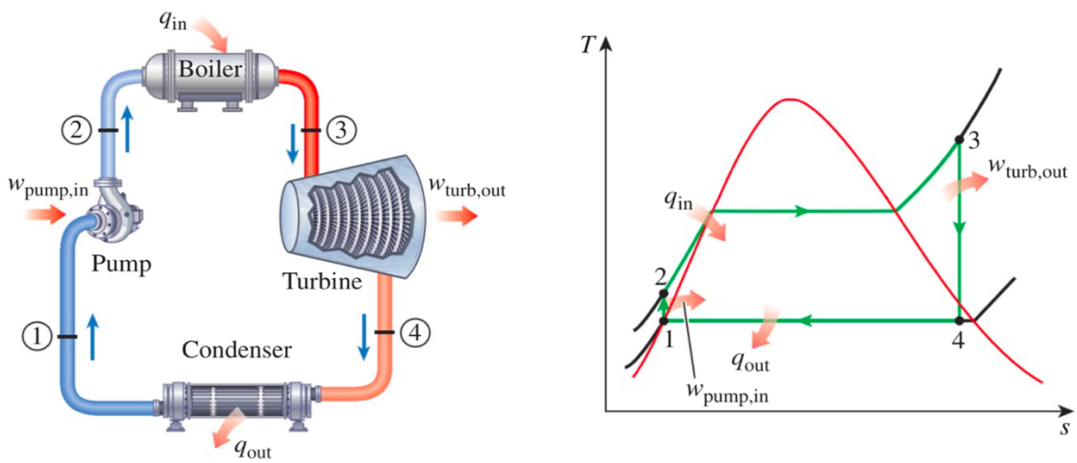


Figure 2.4 Illustration and T-S Diagram of Ideal Rankine Cycle

## 2.3.2 Organic Rankine Cycle

The modeling of Rankine Cycle itself is relatively simple, while the calculation of working fluids is very vital. Even a branch of engineering thermodynamics has been established to calculate the thermal properties of substances. Most of the calculations are designed for pure substances, including inorganic and organic matters. And there are also calculations for binary solutions, like the lithium bromide discussed in the next part, and more complex solutions. Calculation of pure substances will be discussed in chapter 5.

The following table, Table 2.1, Calculation Guide of ORC_R123, is compiled on the basis of thermodynamic property calculation. The cardinal numbers in the first column indicate which status it is. The ordinal numbers in each cell except those set as decision variables indicate the sequence of code. The successes in calculation of ORC_R123, AC_ALB, HP_R410a and VCC_R134a rely heavily on the correctness and feasibility of these calculation guides.

| No | T | p | v | s | h | |
|---|---|---|---|---|---|---|
| 1 | T_1 = x(17) | 2nd. PR Equation | 1st. Saturated Liquid Density Equation | 3rd. CoolProp('T''P') | 3rd. CoolProp('T''P') | Saturated Liquid |
| 2 | 5th. CoolProp('P''H') | DeltaP_ORCp = x(16)<br>p_2 = p_1 + DeltaP_ORCp | 6th. PR Equation | 7th. S_ORC2 = S_ORC1 / EtaS_ORCp; | 4th. H_ORC2 = H_ORC1 + v_ORC1 * DeltaP_ORCp; | - |
| 3 | T_3 = x(15) | 8th. P_3 = P_2 * DeltaP_ORCe | 9th. PR Equation | 10th. CoolProp('T''P') | 10th. CoolProp('T''P') | Overheat Gas |
| 4 | 13th. CoolProp('P','S') | 11th. P_ORC4 = P_ORC1 / DeltaP_ORCc | 14th. PR Equation | 12th. S_ORC4 = S_ORC3 / EtaS_ORCt; | 15th. CoolProp('P','S') | - |
| 1 | T_1 = x(17) | 2nd. PR Equation | 1st. Saturated Liquid Density Equation | 3rd. CoolProp('T''P') | 3rd. CoolProp('T''P') | Saturated Liquid |

Table 2.1 Calculation Guide of ORC_R123

These two are T-s diagram and p-h diagram of ORC_R123, plotted by program in this project, *Plot_GEI_ORC_Exergy*, through MATLAB. The input parameters are **M_ORC = 0.3381**, **T_ORC3 = 473.15**, **P_ORC2 = 506625**, **T_ORC1 = 313.15**.

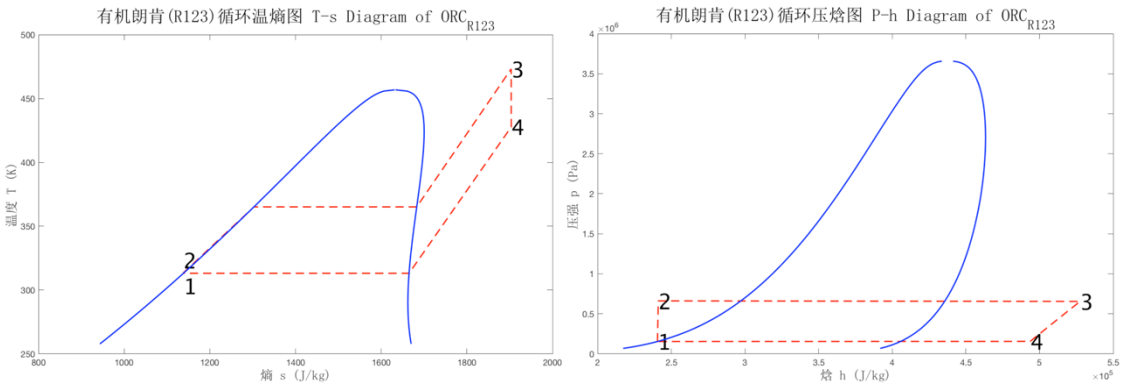


Figure 2.5 T-s Diagram of ORC_R123 plotted by *Plot_GEI_ORC_Exergy*

## 2.4 Refrigeration Cycle

### 2.4.1 Ideal Vapor Compression Refrigeration Cycle

The ideal vapor-compression refrigeration cycle is the same as the rankine cycle in opposite direction.

The refrigerant enters condenser as super-heated vapor at state 2. After rejecting heat to the surroundings, the refrigerant leaves as saturated liquid at state 3. Then, it passes through an expansion valve or capillary tube, with pressure down to evaporator pressure, becoming a low-quality saturated mixture at state 4. And it completely evaporates by absorbing heat from the refrigerated space evaporator, leaving the evaporator as saturated vapor at state 1. Finally, it's compressed isentropically to the condenser pressure in condenser and complete the cycle.

In an ideal vapor-compression refrigeration cycle, the refrigerant enters the compressor at state 1 as saturated vapor and is compressed isentropically to the condenser pressure. The temperature of the refrigerant increases during this isentropic compression process to well above the temperature of the surrounding medium. The refrigerant then enters the condenser as super-heated vapor at state 2 and leaves as saturated liquid at state 3 as a result of heat rejection to the surroundings. The temperature of the refrigerant at this state is still above the temperature of the surroundings.

The saturated liquid refrigerant at state 3 is throttled to the evaporator pressure by passing it through an expansion valve or capillary tube. The temperature of the refrigerant drops below the temperature of the refrigerated space during this process. The refrigerant enters the evaporator at state 4 as a low-quality saturated mixture, and it completely evaporates by absorbing heat from the refrigerated space. The refrigerant leaves the evaporator as saturated vapor and reenters the compressor, completing the cycle.

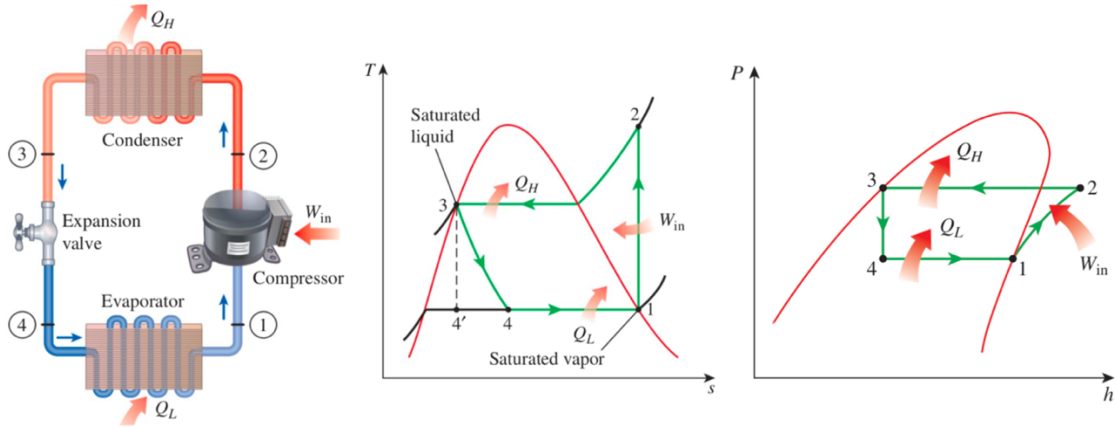


Figure 2.6 a b c, Schematic and T-s diagram for the ideal vapor-compression refrigeration cycle.

## 2.4.2 Ideal Absorption Refrigeration Cycle

The most difficult model to program is that of AC_ALB besides that of MGT, because it involves both the calculations of thermal properties for refrigerant and thermal properties for lithium-bromide solution, which are both discussed in chapter 5.

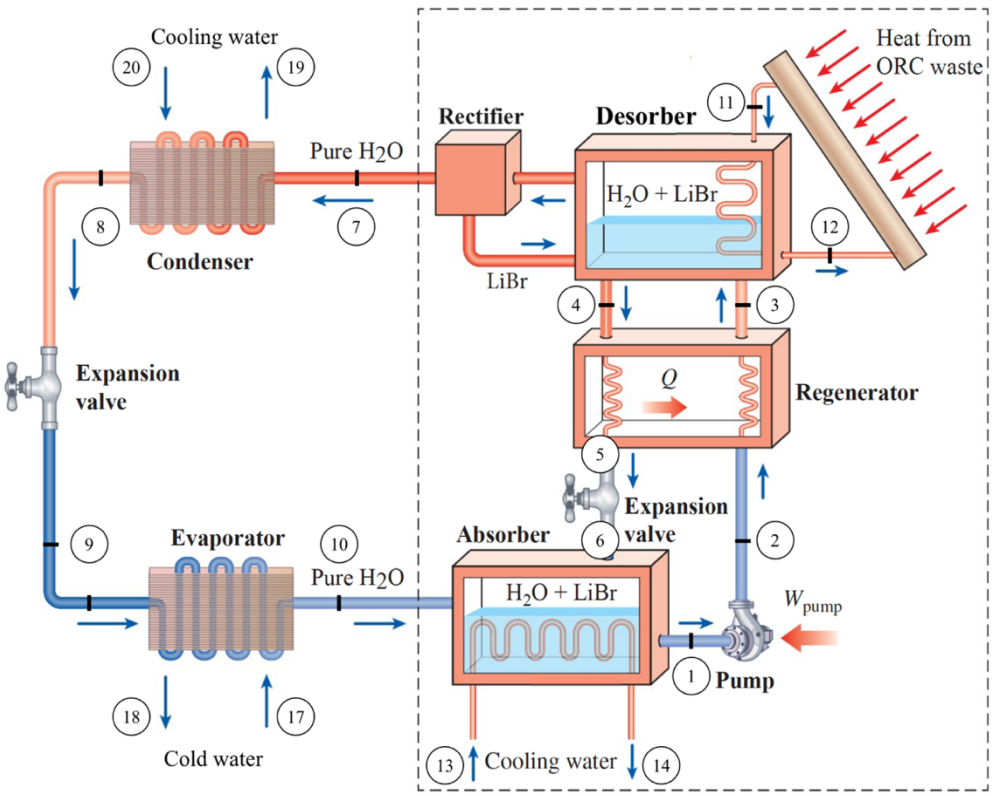


Figure 2.7 Schematic for Aqueous Lithium-Bromide Absorption Chiller

H2O vapor leaves the evaporator and enters the absorber, where it dissolves and reacts with LiBr to form H2O-LiBr, which is an exothermic reaction; thus heat is released during this process. The amount of H2O that can be dissolved in LiBr is inversely proportional to the temperature. Therefore, it is necessary to cool the absorber to maintain its temperature as low as possible, hence to maximize the amount of H2O dissolved in LiBr. The liquid H2O-LiBr solution, which is rich in H2O, is then pumped to the generator. Heat is transferred to the solution from a source to vaporize some of the solution. The vapor, which is rich in H2O, passes through a rectifier, which separates the LiBr and returns it to the generator. The high-pressure pure H2O vapor then continues its journey through the rest of the cycle. The hot H2O-LiBr solution, which is weak in H2O, then passes through a regenerator, where it transfers some heat to the rich solution leaving the pump, and it is throttled to the absorber pressure.

If the absorption refrigeration cycle is divided into two parts according to imaginary-line box in Figure 2.7, tubes in the left parts only contains pure refrigerant, while the right part contains solution in different concentration. So, we define the left parts as refrigerant cycle and the right parts as solution cycle. The solution cycle as a whole helps the refrigerant cycle to continue by absorbing the liquid refrigerant and regenerate vapor refrigerant. This process requires power, so we can treat the solution cycle as a reversible heat engine, shown in Figure 2.8.

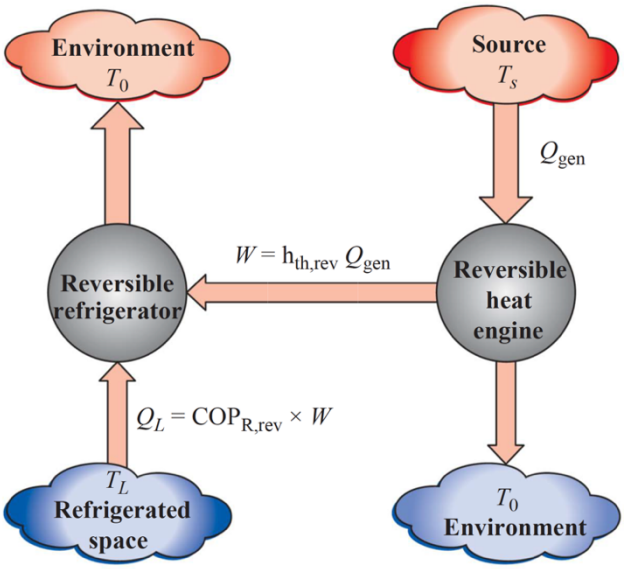


Figure 2.8 Illustration of Principle of Absorption Refrigeration Cycle

This is the T-s diagram and p-h diagram of AC_ALB plotted by program in this project *Plot_GEI_AC_Exergy*, through MATLAB. The input parameters are **`T_AC10 = 274.45`**, **`T_AC8 = 303.35`**, **`y_1 = 0.5322`**, **`y_4 = 0.6711`**, **`M_AC1 = 4.28417E-2`**, **`Eta_shx = 0.64`**.

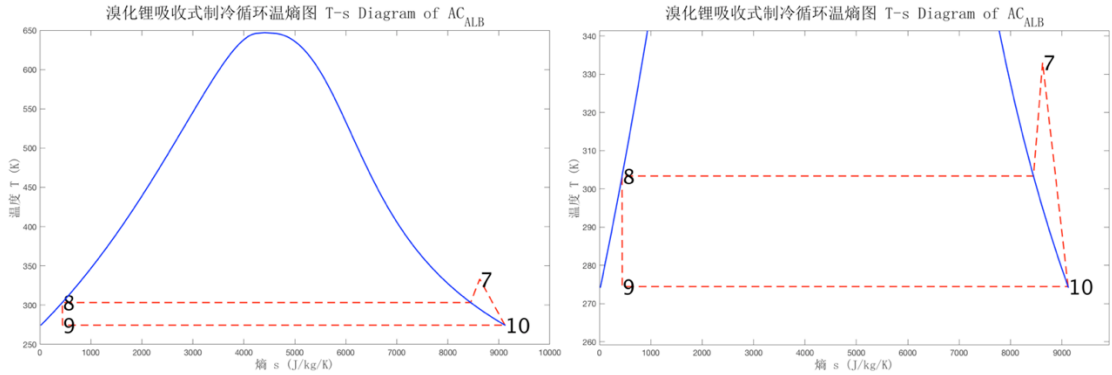


Figure 2.9 T-s Diagram of AC_ALB plotted by *Plot_GEI_AC_Exergy*

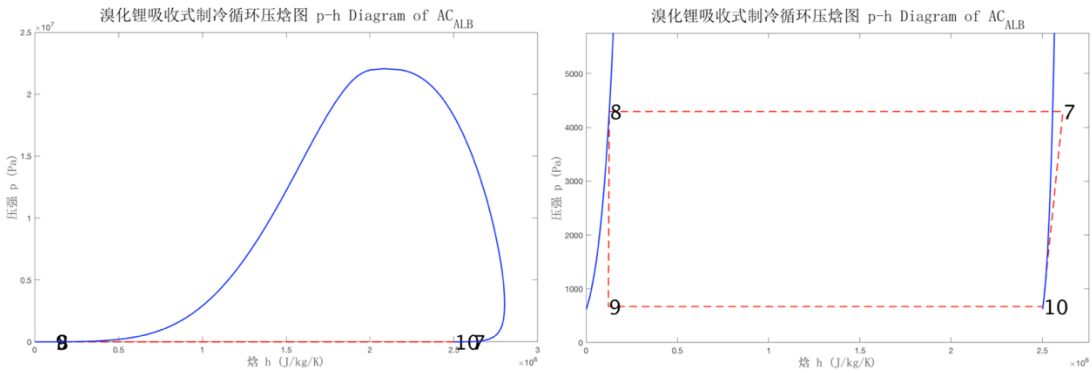


Figure 2.10 p-h Diagram of AC_ALB plotted by *Plot_GEI_AC_Exergy*

## 2.4.3 Absorption Cycle & Vapor Compression Cycle

If the analogy of absorber and generator as heat engine providing power is accepted, we can compare the absorption refrigeration cycle with vapor compression refrigeration cycle, and it's obvious the difference only exits in heat engine and pump. In other word, there is no difference in refrigerant cycle between absorption refrigeration cycle and vapor compression refrigeration cycle, which is shown in Figure 2.11.

A further discussion about solution cycle in absorption refrigeration cycle reveals that it can be interpreted by rankine cycle, which is also shown in Figure 2.11. This reasoning simplifies the modeling of absorption refrigeration cycle by modeling refrigerant cycle first and then solution cycle.

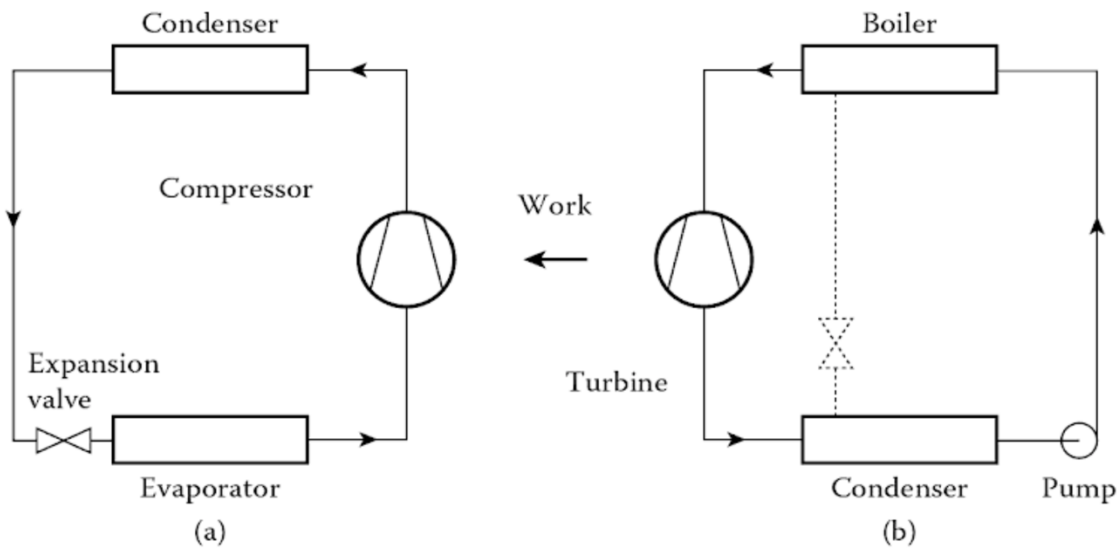


Figure 2.11 a b Illustration of two combined Rankine cycle (a, refrigeration b, power generation).

## 2.5 Ideal Heat Pump Cycle

Heat pumps are generally more expensive to purchase and install than other heating systems, but they save money in the long run in some areas because they lower the heating bills. Despite their relatively higher initial costs, the popularity of heat pumps is increasing. The cycle process is shown in Figure 2.12.

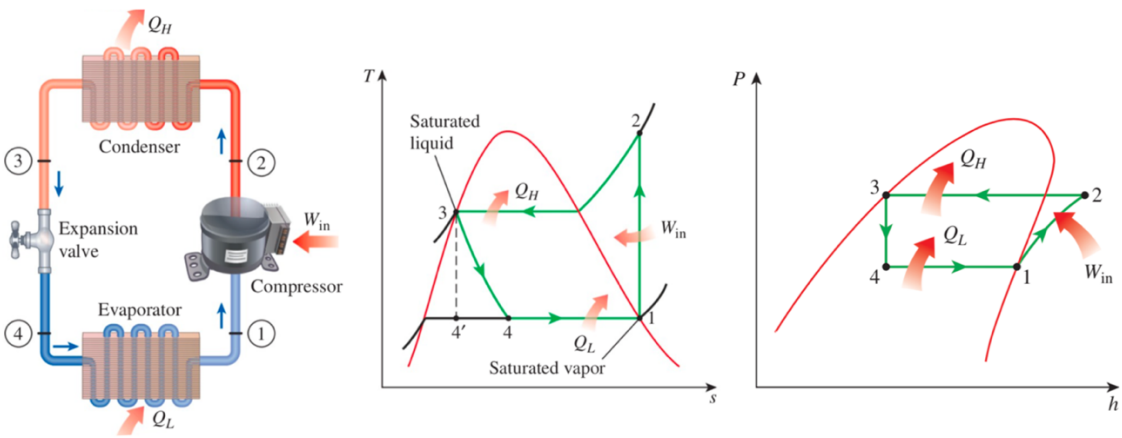


Figure 2.12 a b c Diagrams of HP_R410a

Heat pumps and air conditioners have the same mechanical components. Therefore, it is not economical to have two separate systems to meet the heating and cooling requirements of a building. One system can be used as a heat pump in winter and an air conditioner in summer. This is accomplished by adding a reversing valve to the cycle. As

a result of this modification, the condenser of the heat pump (located indoors) functions as the evaporator of the air conditioner in summer. Also, the evaporator of the heat pump (located outdoors) serves as the condenser of the air conditioner. This feature increases the competitiveness of the heat pump. Such dual-purpose units are commonly used in motels, but it's not discussed in this project.

This is the T-s diagram and p-h diagram plotted by model in this project, *Plot_GEI_HP_Exergy*, through MATLAB. The input parameters are **`M_MP = 1.0`**, **`T_HP3 = 473.15`**, **`p_HP2 = 3039750.0`**, **`T_HP1 = 353.15`**.

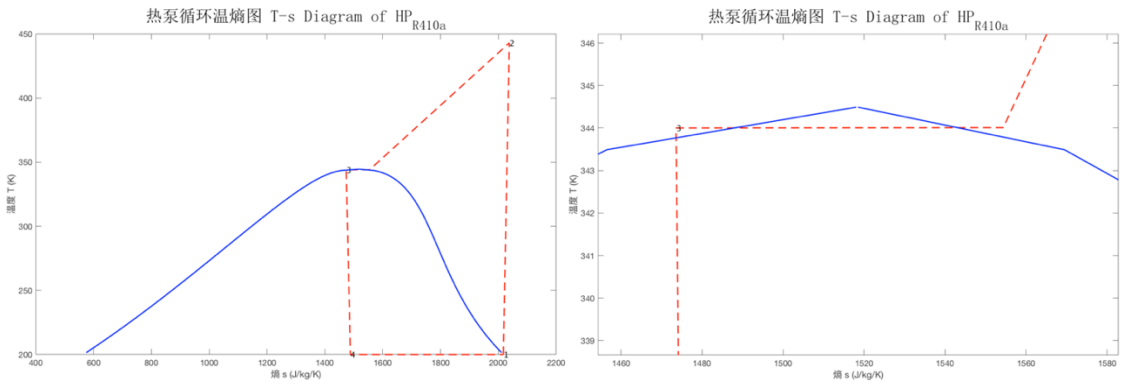


Figure 2.13 T-s Diagram of HP_R410a plotted by *Plot_GEI_HP_Exergy*

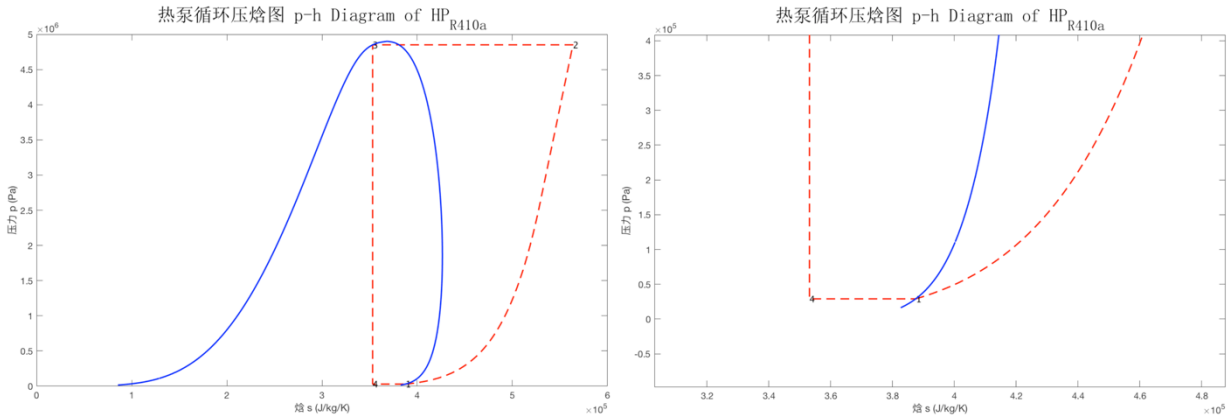


Figure 2.14 p-h Diagram of HP_R410a plotted by *Plot_GEI_HP_Exergy*

# Chapter 3 Integration of Thermal Systems

## 3.1 Exergy Analysis of Thermal Systems

### 3.1.1 Exergy Equation

Exergy can be divided into four distinct components. The two important ones are the physical exergy and chemical exergy. In this study, the two other components which are kinetic exergy and potential exergy are considered negligible as the elevation and speed have negligible changes. The physical exergy is defined as the maximum theoretical useful work obtained as a system interacts with an equilibrium state. The chemical exergy is associated with the departure of the chemical composition of a system from its chemical equilibrium. The chemical exergy is an important part of exergy in combustion process. Therefore, the following exergy balance equation is written:

$$\dot{\mathrm{Ex}}_Q + \sum_i \dot{m}_i e_i = \sum_e \dot{m}_e e_e + \dot{\mathrm{Ex}}_W + \dot{\mathrm{Ex}}_D$$

where subscripts e and i are the specific exergy of control volume inlet and outlet flow and $\mathrm{Ex_D}$, is the exergy destruction. Other terms in this equation are:

$$\dot{\mathrm{Ex}}_Q = \left(1 - \frac{T_0}{T_i}\right)\dot{Q}_i$$

$$\dot{\mathrm{Ex}}_W = \dot{W}$$

$$\mathrm{ex_{ph}} = (h - h_0) - T_0(S - S_0)$$

where $\mathrm{Ex_Q}$ and $\mathrm{Ex_W}$ are the corresponding exergy of heat transfer and work which cross the and boundaries of the control volume, T is the absolute temperature (K) and (0) refer to the ambient conditions respectively. In equation (16), term Ex is defined as follow:

$$\dot{\mathrm{Ex}} = \dot{\mathrm{Ex}}_{ph} + \dot{\mathrm{Ex}}_{ch}$$

For the cycle performance simulation, it was assumed that the system reaches a steady state, and pipe pressure drop and heat losses to the environment in the evaporator, condenser, turbine and pump are neglected. Because of the thermodynamic irreversibility occurring in each of the components, such as non-isentropic expansion, non-isentropic compression and heat transfer over a finite temperature difference, the exergy analysis method is employed to evaluate the performance for low grade waste heat recovery. Consider $P_0$ and $T_0$ to be the ambient pressure and temperature as the specified dead reference state. The exergy of the state point can be considered as

$$E_i = m[(h_1 - h_0) - T_0(s_i - s_0)]$$

The exergy balance for an open thermodynamic system can be expressed as:

$$\sum E_{\text{input}} - \sum E_{\text{output}} = I$$

### 3.1.2 Physical Exergy

Weighted average of the physical exergy of components can be treated as the physical exergy of mixtures. The calculation of the physical exergy of gas in MGT status 6 is expressed by the code below.

```
% Calculate tHe h, s, E_ph of gas in status 6.
H_a6 = CoolProp.PropsSI('H', 'T', T_6, 'P', P_6, 'Air');
S_a6 = CoolProp.PropsSI('S', 'T', T_6, 'P', P_6, 'Air');
H_H6 = CoolProp.PropsSI('H', 'T', T_6, 'P', P_6, 'Water');
S_H6 = CoolProp.PropsSI('S', 'T', T_6, 'P', P_6, 'Water');
H_C6 = CoolProp.PropsSI('H', 'T', T_6, 'P', P_6, 'CarbonDioxide');
S_C6 = CoolProp.PropsSI('S', 'T', T_6, 'P', P_6, 'CarbonDioxide');
H_N6 = CoolProp.PropsSI('H', 'T', T_6, 'P', P_6, 'Nitrogen');
S_N6 = CoolProp.PropsSI('S', 'T', T_6, 'P', P_6, 'Nitrogen');
H_g7 = Ma_x/Mg * H_a6 + (Ma-Ma_x)/Mg * y_H*18/MgC * H_H6 + ...
       (Ma-Ma_x)/Mg * y_C*44/MgC * H_C6 + (Ma-Ma_x)/Mg * y_N*28/MgC * H_N6;
S_g6 = Ma_x/Mg * S_a6 + (Ma-Ma_x)/Mg * y_H*18/MgC * S_H6 + ...
       (Ma-Ma_x)/Mg * y_C*44/MgC * S_C6 + (Ma-Ma_x)/Mg * y_N*28/MgC * S_N6;
E_MGT6 = (H_g7 - H_g0) - T_0 * (S_g6 - S_g0)
```

### 3.1.3 Chemical Exergy

If the $T_0$ is determined, the chemical exergy for diffusion of each component in mixture is a constant. Then the whole chemical exergy of mixture can be calculated by the equation below.

$$\mathrm{ex}_{\text{mix}}^{\text{ch}} = \left[\sum_{i=1}^{n} X_i \mathrm{ex}^{\text{ch}_i} + RT_0 \sum_{i=1}^{n} X_i \operatorname{Ln} X_i\right]$$

For the evaluation of the fuel exergy, the above equation cannot be used. Thus, the corresponding ratio of simplified exergy is defined as the following:

$$\xi^* = \mathrm{ex}_{\mathrm{f}}/\mathrm{LHV}_{\mathrm{f}}$$

Due to the fact that for the most of usual gaseous fuels, the ratio of chemical exergy to the LHV is usually close to 1, one may write:

$$\xi^*_{\mathrm{CH_4}} = 1.06$$
$$\xi^*_{\mathrm{H_2}} = 0.985$$

For gaseous fuel with $C_xH_y$, the following relation is used to calculate:

$$\xi^* = 1.033 + 0.0169\frac{y}{x} - \frac{0.0698}{x}$$

A further assumption can be made to unify the calculation of chemical exergy of fuel,

that is to be represented by High Heat Value (HHV). This method is applied in this project and the corresponding code is show below.

```
% Calculation of HHV of fuel.
R_w = (2257.2 * 1000);                          % J/kg, latent heat of vaporization
HHV = LHV + 1000/16 * n_gC * y_H * 18/1000 * R_w; % J/kg
Ech_f = HHV;
```

### 3.1.4 Exergy Efficiency

There are various methods to compute the exergy destruction and exergy efficiency. They have the same ideas, but they are different from each other. And it can be wrong if it's not expressed correctly. Calculations of exergy destruction and efficiency of components in MGT and overall exergy analyses of MGT are shown below.

```
%% 5.1.5 Exergy Analysis of MGT.
Ed_MGTac = Wp_MGTac + Ma * E_MGT1 - Ma * E_MGT2;
Ed_MGTre = (E_MGT2 * Ma + E_MGT5 * Mg) - (E_MGT3 * Ma + E_MGT6 * Mg);
Ed_MGTcc = (E_MGT3 * Mg + Ech_f * Mf) - E_MGT4 * Mg;
Ed_MGTt = E_MGT4 * Mg - (Wp_MGTt + E_MGT5 * Mg);
Ed_MGThrsg = (E_MGT8 * Ms_MGT + E_MGT6 * Mg) - (E_MGT9 * Ms_MGT + E_MGT7 * Mg);
% Exergy efficiency of components of MGT.
PhiE_MGTcc = (E_MGT4 * Mg - E_MGT3 * Mg) / (Ech_f * Mf);
PhiE_MGTt = Wp_MGTt / (E_MGT4 * Mg - E_MGT5 * Mg);
PhiE_MGTac = (E_MGT2 - E_MGT1) * Ma / Wp_MGTac;
PhiE_MGTre = (E_MGT3 * Ma - E_MGT2 * Ma) / (E_MGT5 * Mg - E_MGT6 * Mg);
PhiE_MGThrsg = (E_MGT9 * Ms_MGT - E_MGT8 * Ms_MGT) / (E_MGT6 * Mg - E_MGT7 * Mg);
% Overall exergy destruction in MGT.
Ed_MGT = Ed_MGTac + Ed_MGTre + Ed_MGTcc + Ed_MGTt + Ed_MGThrsg;
PhiE_MGTp = Wp_MGTt / (Ech_f * Mf + Wp_MGTac + E_MGTm0 * Mg + E_MGT8 * Ms_MGT -
E_MGT7 * Mg - E_MGT9 * Ms_MGT);
PhiE_MGTs = (E_MGT9 * Ms_MGT - E_MGT8 * Ms_MGT) / (Ech_f * Mf + Wp_MGTac +
E_MGTm0 * Mg - E_MGT7 * Mg - Wp_MGTt);
PhiE_MGT = PhiE_MGTp + PhiE_MGTs;
```

The exergy analyses of electricity-driven devices are quite different from that of heat-driven ones.

```
% Exergy damage of gas turbine in ORC_R123.
WP_ORCt = M_ORC * (H_ORC3 - H_ORC4);
We_ORCt = WP_ORCt * EtaG_ORCt;
Ed_ORCt = E_ORC3 * M_ORC - (E_ORC4 * M_ORC + We_ORCt);
PhiEe_ORCt = We_ORCt / (E_ORC3 * M_ORC - E_ORC4 * M_ORC);
```

```
% 5.3.6 Exergy destruction and efficiency of pump in HP_R410a.
We_HPp = M_HP * (H_HP2 - H_HP1);
Ed_HPp = We_HPp - (E_HP2 * M_HP - E_HP1 * M_HP);
PhiE_HPp = (E_HP2 * M_HP - E_HP1 * M_HP) / We_HPp;
```

There are other difficulties in the analyses of desorber and absorber in AC_ALB, for three outlet streams for three inlet streams respectively. Although it's not hard to write code about them, the results haven't been proven right, and it needs further attention.

```
% Exergy destruction and efficiency of desorber in AC_ALB.
Ed_ACd = (E_AC11 * Mg + E_AC3 * M_AC3) - ...
         (E_AC7 * M_AC7 + E_AC12 * Mg + E_AC4 * M_AC4);
PhiE_ACd = (E_AC7 * M_AC7 + E_AC4 * M_AC4 - E_AC3 * M_AC3) / ...
           (E_AC11 * Mg - E_AC12 * Mg);
```

The analysis can be expressed by bar charts of exergy destructions and exergy efficiencies. On the basis of those result, exergy stream chart can also be plotted. Figure 3.1, 3.2, 3.3 is plotted by program in this project, *Plot_GEI_MGT_Exergy*, through MATLAB. **P_2 = 637317.19**, **Eta_MGTac = 0.8988861**, **Eta_MGTt = 0.923143**, **T_3 = 699.999574**, **T_4 = 1100**.

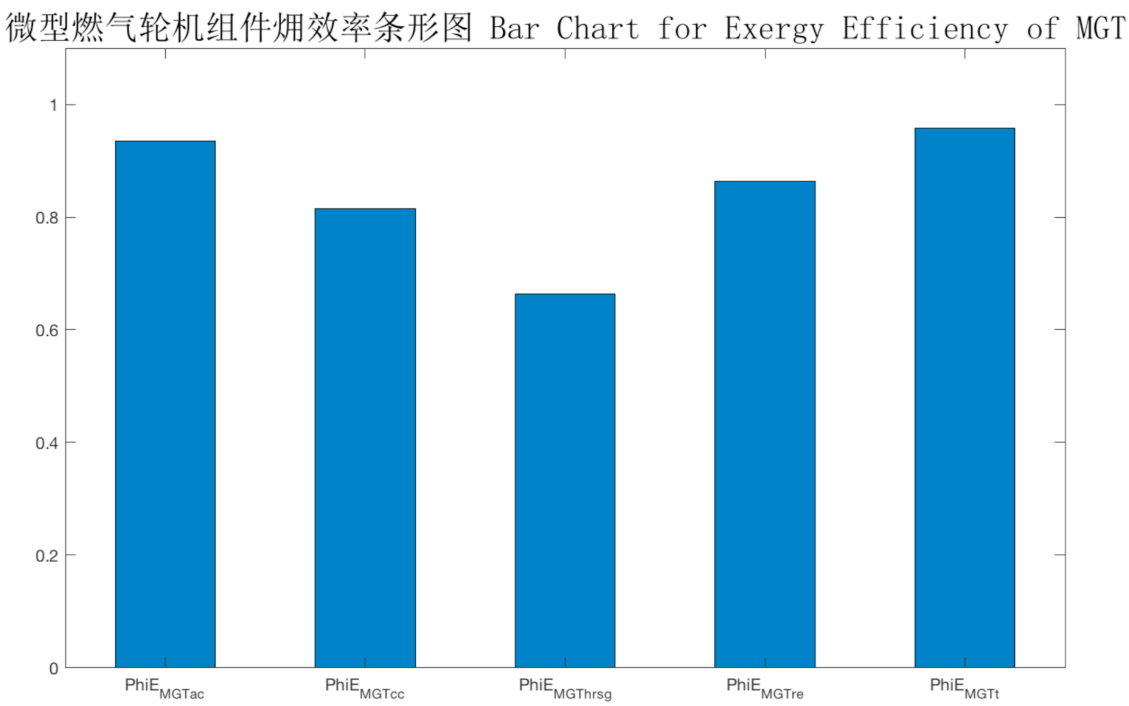


Figure 3.1 Bar Chart for Exergy Efficiency of MGT

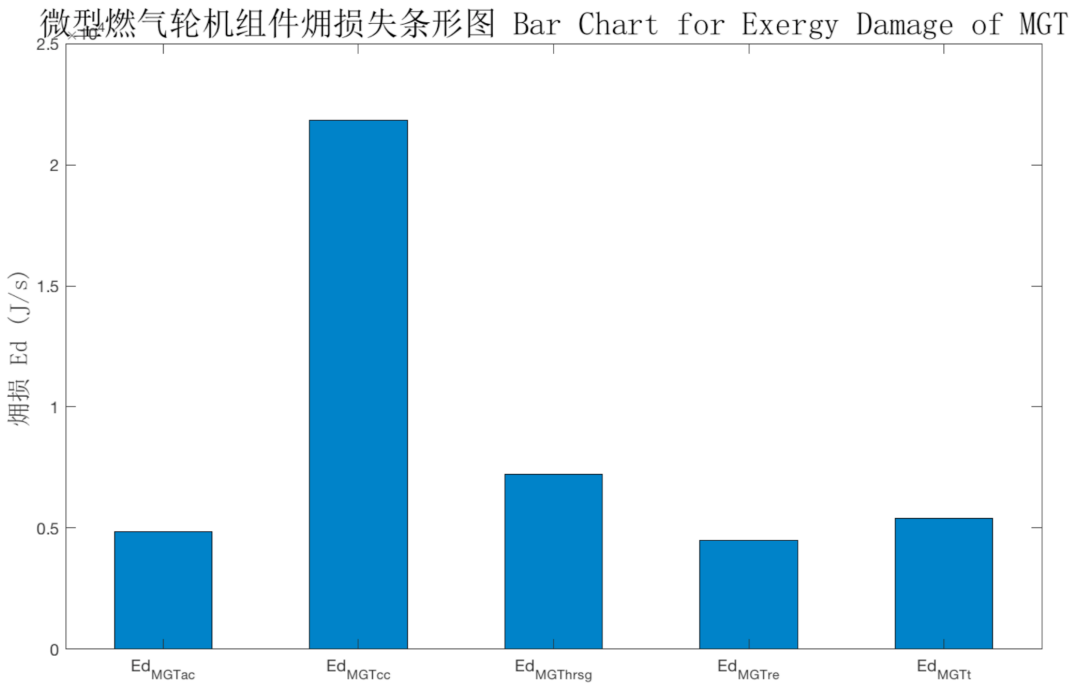


Figure 3.2 Bar Chart for Exergy Destruction of MGT

Five segments in 7th column of exergy stream chart shows the exergy flowing to different substances. Reg segment represents exergy in saturated steam. Green segment represents that in power. And orange segment represents that in waste gas. Determination of heat-power/cold-power ratio and temperature of waste gas are expressed in ratios among those three segments.

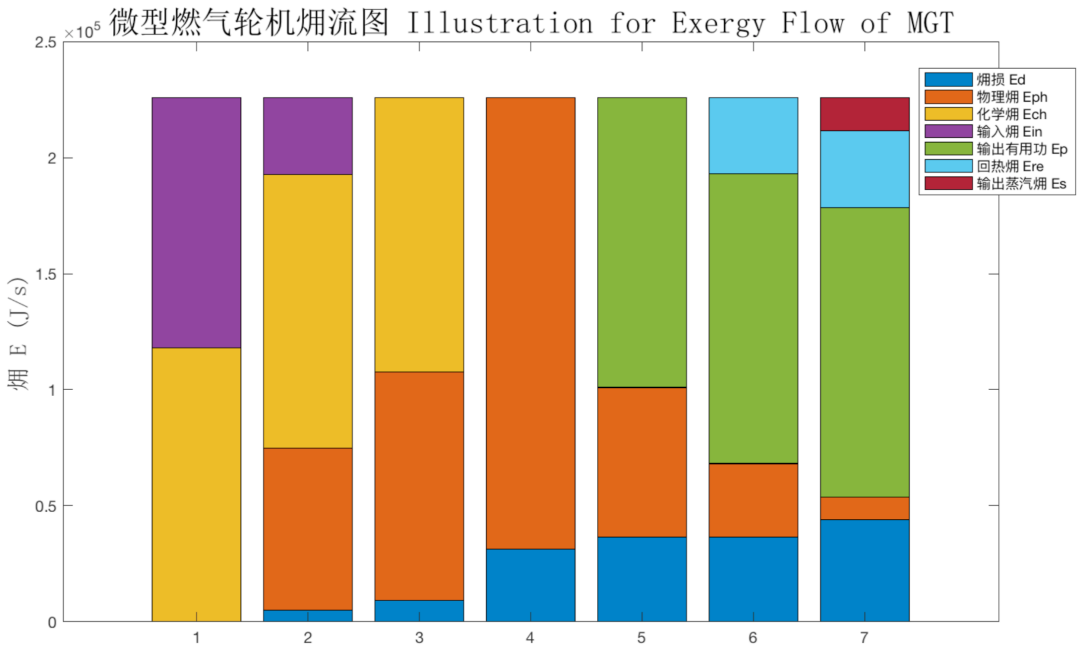


Figure 3.3 Illustration for exergy flow of MGT

## 3.2 Principle of Cascading Utilization

It's obvious in the following Table 3.1 that temperatures of status point in different devices must obey the relative relationships according to principle of heat transfer. And it reveals the importance of waste heat staying in high temperature, so cascading utilization is necessary in increasing overall efficiency.

| Equipment | Hot Steam Inlet Temp | Hot Steam Outlet Temp | Cold Steam Inlet Temp | Cold Steam Outlet Temp | Constraint |
|---|---|---|---|---|---|
| Desorber, AC_ALB | T_AC11 (T_7) | T_AC12 (T_ORC19) | T_AC3 | T_AC4 | c(11) = T_AC4 - T_AC11;<br>c(12) = T_AC3 - T_AC12; |
| Absorber, AC_ALB | T_AC6 | T_AC1 | T_AC13 (T_0) | T_AC14 (T_0H) | c(15) = T_AC14 - T_AC6;<br>c(16) = T_AC13 - T_AC1; |
| Evaporator, AC_ALB | T_AC17 (T_0) | T_AC18 (T_cw) | T_AC9 | T_AC10 | c(13) = T_AC10 - T_AC17;<br>c(14) = T_AC9 - T_AC18; |
| Condensor, AC_ALB | T_AC7 | T_AC8 | T_AC15 (T_0) | T_AC16 (T_0H) | c(17) = T_AC16 - T_AC7;<br>c(18) = T_AC15 - T_AC8; |
| Evaporator, ORC_R123 | T_ORC19 (T_AC12) | T_ORC20 (T_wg) | T_ORC2 | T_ORC3 | c(21) = T_ORC3 - T_ORC19;<br>c(22) = T_ORC2 - T_ORC20; |
| Condensor, ORC_R123 | T_ORC4 | T_ORC1 | T_0 | T_0H | c(23) = T_0H - T_ORC4;<br>c(24) = T_0 - T_ORC1; |
| Evaporator, HP_R410a | T_0 | T_0L | T_HP4 | T_HP1 | c(27) = T_HP4 - T_0L;<br>c(28) = T_HP1 - T_0; |
| Condensor, HP_410a | T_HP2 | T_HP3 | T_8 | T_s | c(29) = T_s - T_HP2;<br>c(30) = T_8 - T_HP3; |
| Evaporator, VCC_R134a | T_0 | T_cw | T_VCC4 | T_VCC1 | c(35) = T_VCC1 - T_0;<br>c(36) = T_VCC4 - T_cw; |
| Condensor, VCC_R134a | T_VCC2 | T_VCC3 | T_0 | T_0H | c(33) = T_0H - T_VCC2;<br>c(34) = T_0 - T_VCC3; |

Figure 3.1 Relative relationship between temperatures in heat exchanger and corresponding constraints

Generally speaking, thermal energy is released from fossil fuel combustion and is then transformed into work in traditional thermal cycles. Thus, how to make effective use of thermal energy after fuel combustion is the key subject in traditional thermodynamic researches. Development of traditional thermodynamics (namely exploitation of thermal cycles) is considered as the process that promotes thermal efficiency conforming to the

principle of cascade utilization of physical energy.

Most thermal cycles and refrigeration cycles work at different temperature ranges. The temperature range of thermal cycle is usually above the ambient temperature; and that of refrigeration cycle providing cryogenic energy for air-conditioning or refrigeration is usually below the ambient temperature. Since thermal cycle and refrigeration cycle are indispensable in the CCHP system, the close interaction between them is very important in system integration. In traditional thermal cycles, thermal efficiency can be improved by increasing the initial temperature or by decreasing the mean temperature in the process of heat release. The exhausted and residual heat with low temperature can act as the high-temperature heat source of an absorption refrigeration cycle through the combination of thermal cycle and refrigeration cycle, and the residual cryogenic energy of the refrigeration cycle can have positive impact on thermal cycle, for example, cooling the inlet flow of the compressor.

The T-s diagram and temperature change of MGT, AC and ORC in Green Energy Island is plotted by program in this project, *Plot_GEI_Exergy*, with decision variables the same as previous conditions.

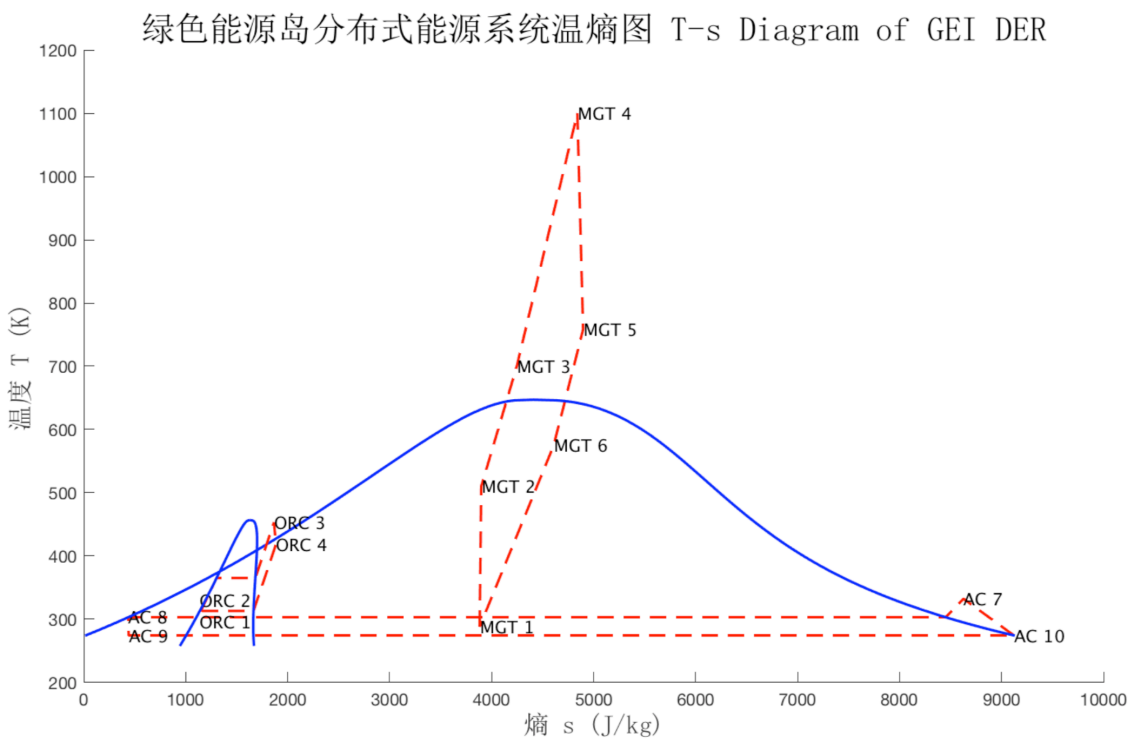


Figure 3.4 T-s Diagram of GEI DER System

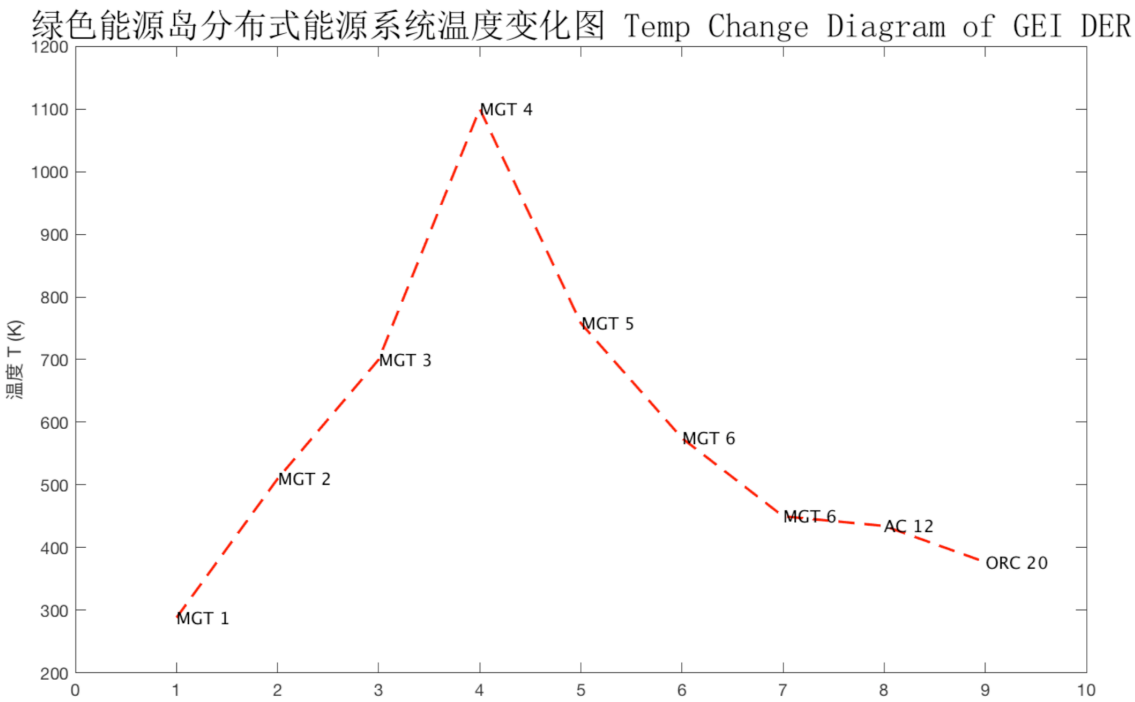


Figure 3.5 Temperature Change Diagram of GEI DER System

In summary, as complementary to each other, thermal cycle and refrigeration cycle can be integrated in the CCHP system. Besides independent consideration given to cascade utilization of physical energy in thermal cycle or refrigeration cycle, special attention should be paid to the coupling between thermal cycle and refrigeration cycle in the CCHP system integration.

## 3.3 Principle of Multi-Energy Complementation

Lots of thermal energy with different energy levels as well as electricity is needed in our daily life. In traditional energy systems, electricity is supplied from the electricity grid (mainly from steam power plants), heating loads come from different styles of boilers, and most air-conditioning cooling loads come from electric chillers. In this mode, different demands are satisfied by different single cycles, and the performance of each system is determined by the performance of single cycles. Since it is rather difficult to further improve the performance of single systems, and a great deal of thermal energy needs to be exchanged in thermal cycles, the heating systems and the cooling systems with the power systems in the combined cooling, heating and power (CCHP) system could be integrated. This system can distinguish and utilize thermal energy in light of different energy levels based on the principle of cascade utilization of physical energy. Hence, exergy losses of each process decrease and total system performance improves

obviously.

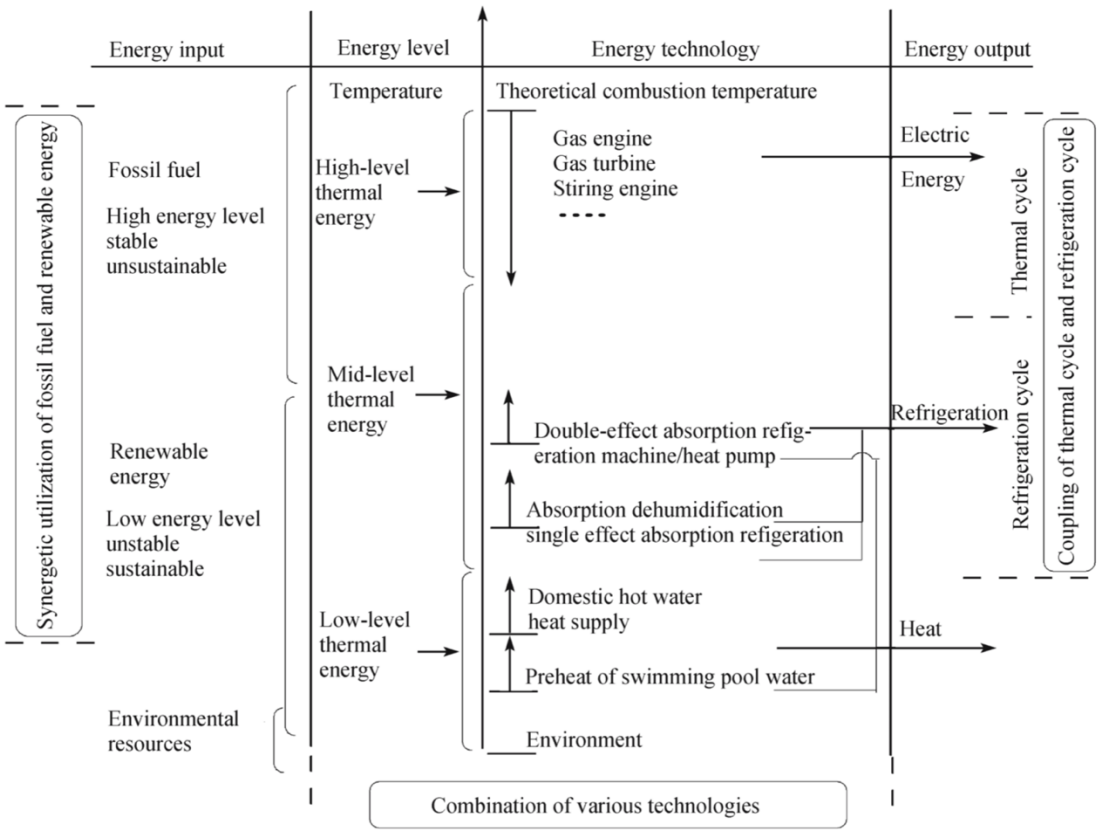


Figure 3.6 Illustration of Cascading Utilization and Multi-Energy Complementation

Based on the characteristics of renewable energy as dispersal distribution and small scale, the CCHP system can be one preferable way to use renewable energy effectively. Solar energy, geothermal energy and bio-fuel can be utilized in the CCHP system. In some cases, thermal energy from the environment, the atmosphere and water resources, also can act as the energy input of the CCHP system. However, compared with fossil fuel, renewable energy, especially solar energy, has bad continuity (instability) and low energy level (or low energy density) etc., which are the major obstacles to their effective utilization. In addition, there are few CCHP systems solely using renewable energy due to the great investment cost.

Several available technologies that can be used in the CCHP system are shown in Figure 3.6, including thermal engines, absorption refrigerator, and absorption dehumidification, etc. The CCHP system synthesis should be based on the cascade utilization of thermal energy. Fossil fuel is usually burnt directly in the CCHP system, and thermal energy with high temperature will be released in the combustion process.

High-temperature thermal energy can be first used in engines, such as gas engine, gas turbine and Stirling engine, to generate electricity for building demands. The temperature of the exhaust of the engine is in the range of 400°C to 600°C, and the surplus heat (mid-temperature thermal energy) can be recovered to drive a double-effect absorption refrigerator or heat pump and generate cryogenic energy or thermal energy for the building's cooling or heating load. Since the thermal energy with a temperature lower than 170°C cannot be used with current double-effect absorption refrigerators, part of the low-temperature thermal energy, whose temperature is higher than 90°C, can be recovered and used to generate hot water, to drive single-effect absorption refrigerators or dehumidify air in buildings. Surplus thermal energy with a temperature lower than 90°C can also be further used before being discharged to the atmosphere in case of special demands, such as heating swimming pool water. In a word, different methods can be adopted to utilize thermal energy more efficiently according to its temperature. What method should be adopted for certain thermal energy also depends on concrete cooling or heating requirements of the buildings. [18]

The exergy efficiency and destruction of distributed energy system in Green Energy Island is plotted in Figure 3.7 and Figure 3.8, which is accomplished by a program in this project, *Plot_GEI_Exergy*, with decision variables the same as previous conditions.

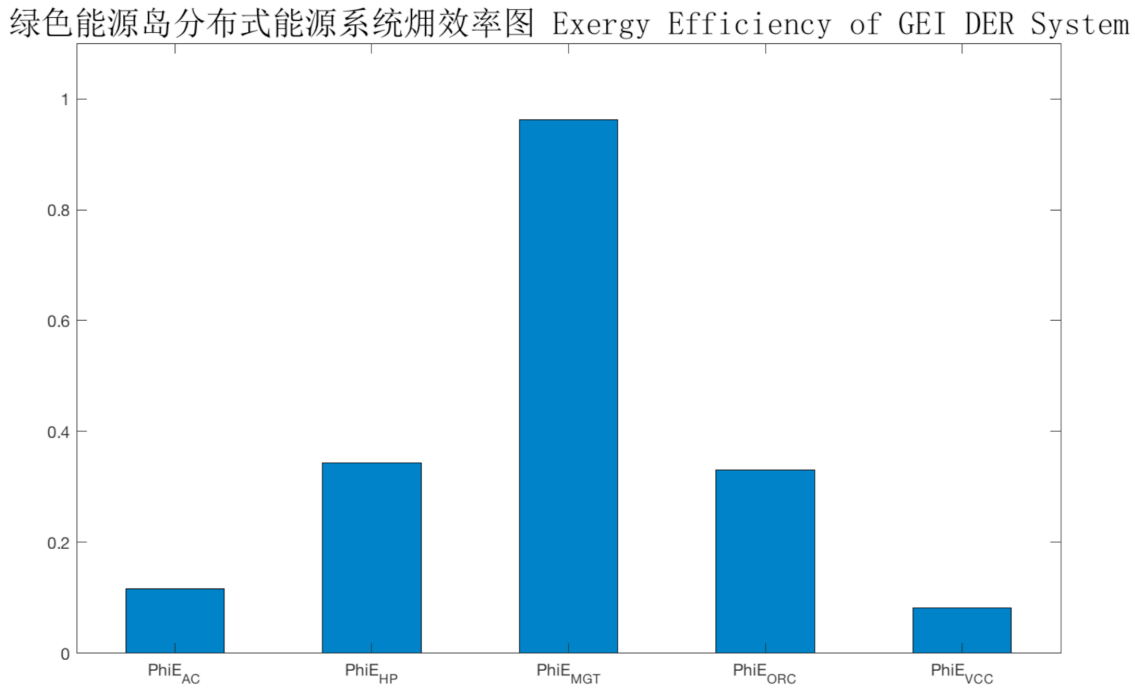


Figure 3.7 Exergy Efficiency of GEI DER System

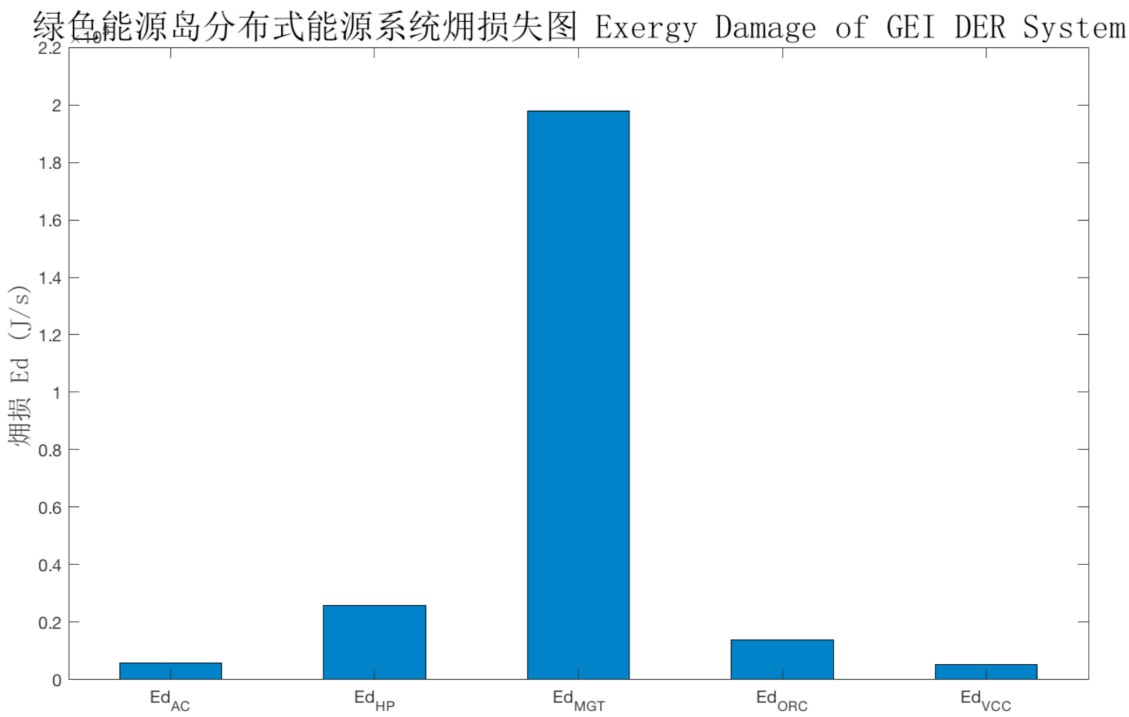


Figure 3.8 Exergy Damage of GEI DER System

It's obvious that though there is much exergy destruction in MGT, the efficiency of MGT is still the highest. And it's the efficiencies of HP_R410a and VCC_R134a that remain lowest, so the cogeneration is more efficient that electrification.

# Chapter 4 Optimization of DER System

## 4.1 Introduction to Optimization

There are many ways to do optimization, shown in Figure 6. In a mixed integer linear programming (MILP) model, the value of the objective function is optimized by changing the values of the decision variables (only integer), object to constraints on the values that the variables can hold. [19]

There are many ways to do optimization, shown in Figure 4.1.

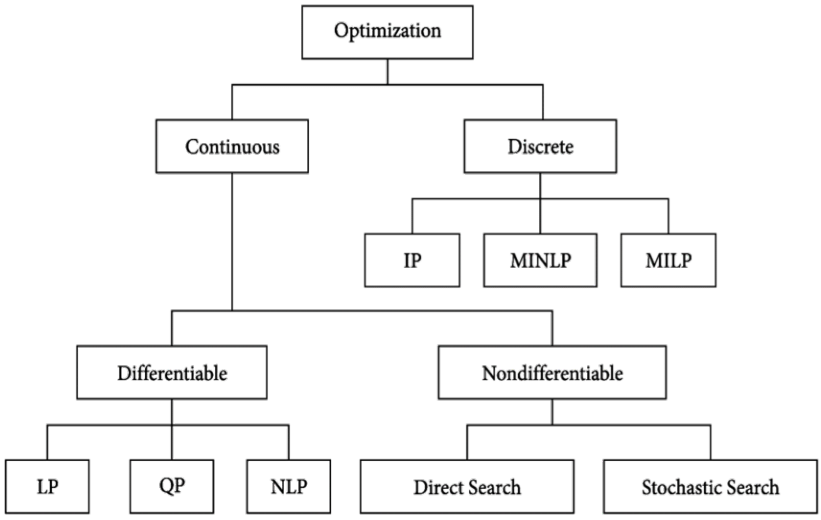


Figure 4.1 Classification of Optimization Method.

The traditional optimization methods. especially gradient methods, Newton's method, conjugate gradient methods, and quasi-Newton methods, starts with an initial point and then generate a sequence of iterates, and the sequences always converge to local minimizers. [20] Moreover, derivatives, even second derivatives in the case of Newton's method, are required, which makes the problem more complicated and the efficiency lower. In contrast, global research algorithms are applicable to much wider class of optimization problems and make the result more accurate, with the help of customized code.

## 4.2 Optimization using Genetic Algorithm

### 4.2.1 Introduction to Genetic Algorithm

Genetic Algorithm (GA) is a probabilistic search method for solving both constrained and unconstrained optimization problems based on a natural selection process that mimics biological evolution strategy. The algorithm repeatedly modifies a population of individual solutions. At each step, the genetic algorithm randomly selects individuals from the current population and uses them as parents to produce the children for the next generation. Over successive generations, the population "evolves" toward an optimal solution.

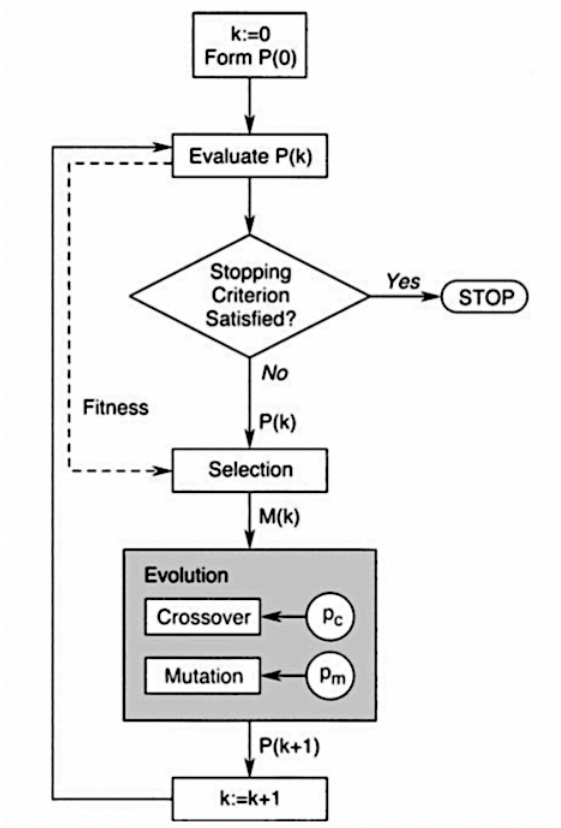


Figure 4.2 Flowchart for genetic algorithm.

The genetic algorithm differs from a classical, derivative-based, optimization algorithm in two main ways, as summarized in the following table.

| Classical Algorithm | Genetic Algorithm |
|---|---|
| Generates a single point at each iteration. The sequence of points approaches an optimal solution. | Generates a population of points at each iteration. The best point in the population approaches an optimal solution. |
| Selects the next point in the sequence by a deterministic computation. | Selects the next population by computation which uses random number generators. |

Because the combinations of decision variables are created before computation, system modeling engineer can program in natural sequence of the problem in most operations, which reduced the amount of work enormously and increase the calculation efficiency. Also, due to its random nature, GA improves the chance of finding a global solution. So, GA is the best tool to find global minima of highly nonlinear engineering problems.

### 4.2.2 Generation, Population and Diversity

An individual is any point which can be applied to the fitness function. A population is an array of individuals. In this research, the size of the population is 30 and the number of variables in the fitness function is 21, so the population can be represented by a 30-by-21 matrix. The same individual may appear more than once in the population. And not all individuals are qualified because of the constraints. At each iteration, the genetic algorithm performs a series of computations including crossover and mutation on the current population to produce a new population. Each successive population is called a new generation. Diversity refers to the average distance between individuals in a population. A population has high diversity if the average distance is large; otherwise it has low diversity.

The first generation, diversity and two computations are all deterministic factors in the whole optimization process, and they are inter-linked with each other. For example, If the first generation is not in low diversity, or crossover factor is relatively small, the global optimal is unlikely to be found out. On the other hand, it can be time-consuming because of the high diversity and crossover factor.

### 4.2.3 Algorithms for Solving Nonlinear Constraint

**Augmented Lagrangian Genetic Algorithm**. By default, the genetic algorithm uses the Augmented Lagrangian Genetic Algorithm (ALGA) to solve nonlinear constraint problems without integer constraints. The Augmented Lagrangian Genetic Algorithm (ALGA) attempts to solve a nonlinear optimization problem with nonlinear constraints,

linear constraints, and bounds. In this approach, bounds and linear constraints are handled separately from nonlinear constraints. A subproblem is formulated by combining the fitness function and nonlinear constraint function using the Lagrangian and the penalty parameters. A sequence of such optimization problems are approximately minimized using the genetic algorithm such that the linear constraints and bounds are satisfied. A subproblem formulation is defined as

$$\Theta(x, \lambda, s, \rho) = f(x) - \sum_{i=1}^{m} \lambda_i s_i \log(s_i - c_i(x)) + \sum_{i=m+1}^{mt} \lambda_i ceq_i(x) + \frac{\rho}{2} \sum_{i=m+1}^{mt} ceq_i(x)^2,$$

where

1. The components λi of the vector λ are nonnegative and are known as Lagrange multiplier estimates
2. The elements si of the vector s are nonnegative shifts
3. ρ is the positive penalty parameter.

Each subproblem solution represents one generation. The number of function evaluations per generation is therefore much higher when using nonlinear constraints than otherwise.

**Penalty Algorithm**. In its evaluation of the fitness of an individual, ga computes a penalty value as follows. If the individual is feasible, the penalty function is the fitness function. If the individual is infeasible, the penalty function is the maximum fitness function among feasible members of the population, plus a sum of the constraint violations of the (infeasible) individual. This method is not used in the process of GA calculation, but its idea is used to reduce the number of unqualified individuals.

## 4.3 Optimization of DER System in GEI

### 4.3.1 Introduction to Optimization of DER System in GEI

Optimization of DER System in GEI can be very complicated because of the various decision variable. There is a difficulty in the correspondence among Mg in MGT, M_AC and M_ORC, which increase the failure rate sharply, because of the big differences in amount and affections in outlet temperatures. So, this multi-component system must be divided into several parts for analysis. Finally, *GEI_Optim_Exergy_GA* program is performed to do the overall optimization.

Figure 4.3 is the illustration of Optimization Model of DER System in GEI, with CST, WT and PV removed. These three components utilize intermittent energy source,

sun light and wind, which determines that they cannot be major parts of DER system. 20% is assumed as their contribution degree in this case, and their rated power can be easily calculated. So, they are neglected in the optimization model.

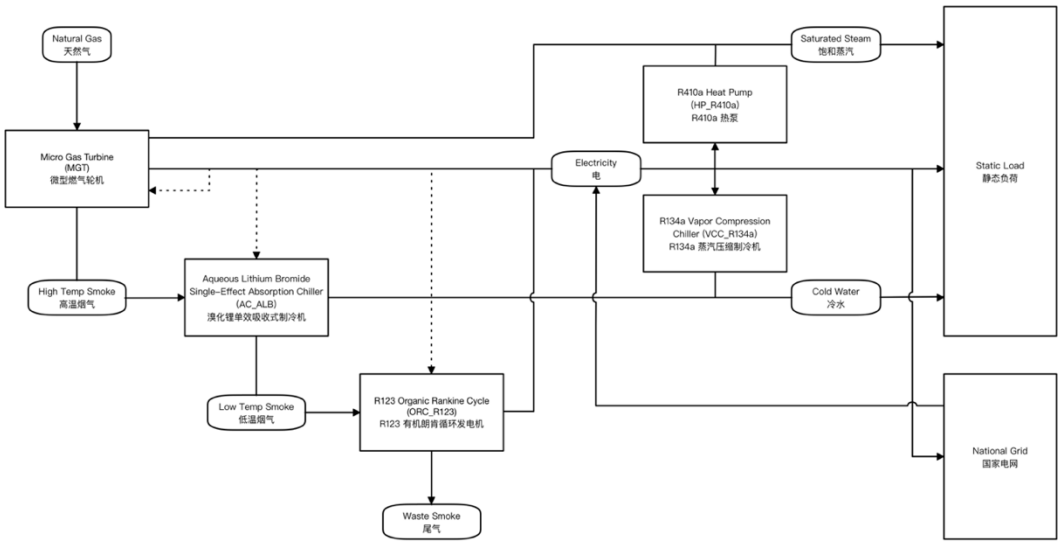


Figure 4.3 Illustration of Optimization Model of DER System in GEI

Optimization Model of DER System in GEI can be further regarded as two parts. HP_R410a and VCC_R134a are driven by electricity provided by MGT and National Grid, so they both have the ability to response to the changing demands in real conditions. But the electricity-driven feature determines that their exergy efficiency is relatively lower, so they are not supposed to be the main source of heat and cold water. Under rated operating condition in this research, some assumptions are made according to which one is chosen as the main product between heat and cold water. Usually, the DER system mainly supply heat in northern area, and mainly supply cold water in southern area. Then, several pre-analyses are performed to define the Heat-Power Ratio or Cold-Power Ratio, and the decision variables concerning fluid rate are computed. Finally, optimization of overall DER system is conducted.

So, there are four MATLAB programs used in this research, other programs for plotting are not listed here:

(1) *MGT_GEI_Optim_Exergy_GA*, genetic algorithm optimization program for Heat-Power Ratio/Cold-Power Ratio and **DV_MGTm**,

(2) *AC_GEI_Optim_Exergy_GA*, calculation program for **DV_ACm**,

(3) *ORC_GEI_Optim_Exergy_GA*, calculation program for **DV_ORCm**,

(4) *GEI_Optim_Exergy_GA*, overall genetic algorithm optimization program.

### 4.3.2 Decision Variables in Optimization of DER System in GEI

There are 21 decision variables in this research. Because three different demands must be met, it can be too time-consuming to find the best combination, even to find a possible combination. So, in this research, decision variables are deliberately sorted into three types: (1) decision variables that defines heat-power ratio, (2) decision variables concerning fluid rate, (3) other decision variables. Decision variables in type 1 and type 2 are restricted in more narraw changing intervals because they have a large impact on temperature change.

It's vital to define Heat-Power Ratio (**RaHP**) or Cold-Power Ratio (**RaCP**) (for northern area and southern area respectively) because of the cogeneration of heat and power. In this case, DER system in GEI, tri-generation of heat, power and cold water makes **RaHP**/**RaCP** more important. And if a "Heat-Cold-Power Ratio" is defined, the mathematical model will become very complicated after re-programmed. Because the "Heat-Cold Ratio" must be used as the proportion of **Ms_MGT** and **Mcw_AC**, the calculation consequences of MGT model and AC_ALB model will be reversed, and calculation of ORC_R123 model will be affected for the change of **T_AC12**.

**RaHP** is easy to be defined as it only involves MGT. According to previous section, the *MGT_GEI_Optim_Exergy_GA* program is performed first, with **Wp_MGT** defined, usually as 50 kW, so **DV_MGTm** can be calculated. Then **T_7** is set with reference to experience, and **Ms_MGT** can be computed by the following equations. Finally, **DV_MGTm** can be computed.

```
% Calculate Ms_MGT_m and DV_MGTm
Ms_MGT_m = (T_6 - T_7) * (Mg_m * Cp_g) / (H_MGT9 - H_MGT8);
DV_MGTm = Ms_MGT / Ms_MGT_m;
```

To define **RaCP** is not too complicated. The first several operation is the same as previous calculation of **RaHP**. Attention should only be paid to **T_7**, because in the southern area supplying primarily cold water, **T_7** is ought to be higher than that in northern area to provide more exergy for AC_ALB. Additionally, **T_AC12** is set with reference to experience, because exergy must be supplied to ORC_R123 and the **T_AC12** cannot be set too low. **T_wg** for the temperature of waste gas is usually set, and **T_AC12** is a middle value between **T_7** and **T_wg**. In this case, the proportion 0.2 is chosen. The

*AC_GEI_Optim_Exergy_GA* program is performed to compute **Mcw_AC_m** and **DV_ACm** in AC_ALB.

```
% Calculate DV_ACm
T_AC11 = T_7; P_AC11 = P_7; P_AC12 = P_AC11;
H_AC11 = H_g7;
Q_ACd_m = M_AC4_m * H_AC4 + M_AC7_m * H_AC7 - M_AC3_m * H_AC3;
T_AC12 = T_AC11 - (T_AC11 - T_wg) * 0.2;
Mcw_AC_m = Q_ACd_m / Cp_g / (T_AC11 - T_AC12) / Mg_m;
DV_ACm = 1 / Mcw_AC_m;
```

### 4.3.3 Fitness Function for Optimization of DER System in GEI

Two methods for solving nonlinear constraint described in section 4.2.3 are both chosen as the solver. Augmented Lagrangian Genetic Algorithm is chosen as main solver in default by MATLAB Genetic Algorithm, and the following codes in *GEI_Optim_Exergy_GA* can serve as the Penalty Algorithm for the electricity deficit, which is caused by the HP_R410a or VCC_R134a to provide enough heat or cold water in case electricity generated cannot satisfy their need.

```
% Fitness Function for Optimization of DER System in GEI
switch Mcw > Mcw_ACe + Mcw_VCCe
  case '1'
    Ed_cw = 2 * (Mcw - Mcw_ACe - Mcw_VCCe);
  case '0'
    Ed_cw = Mcw_ACe + Mcw_VCCe - Mcw;
end
```

Because the lack of economic factors in optimization, exergy destruction minimization is set as the objective function of GEI DER system.

```
% Exergy Destruction Minimization Objective Function
f = Ed_MGT + ... % Ed_MGTac + Ed_MGTre + Ed_MGTcc + Ed_MGTt + Ed_MGTre + ...
    Ed_AC + ...  % Ed_ACa + Ed_ACd + Ed_ACe + Ed_ACc + Ed_ACs + Ed_ACp + ...
    Ed_ORC + ... % Ed_ORCc + Ed_ORCe + Ed_ORCp + Ed_ORCt + ...
    Ed_HP + ...  % Ed_HPc + Ed_HPe + Ed_HPp + ...
    Ed_VCC + ... % Ed_VCCc + Ed_VCCe + Ed_VCCp + ...
    Ed_cw + Ed_s + Ed_e;
```

# Chapter 5 Thermal Properties of Working Substances

## 5.1 Introduction to Thermal Property

To illustrate the use of the balance equations in the simplest manner, examples were given using either ideal gases or fluids whose thermodynamic properties were available in graphical and tabular form. Unfortunately, no gas is ideal over the whole range of pressure and temperature, and thermodynamic properties tables are not always available, so a necessary ingredient of many thermodynamic computations is the calculation of the thermodynamic properties of real substances in any state. The main topic of this chapter is establishing how to solve thermodynamic problems for real substances given heat capacity data and the relationship between pressure, volume, and temperature.

## 5.2 Equation of State

### 5.2.1 Introduction to Equation of State

Clearly, to use Eqs. 6.2-19 through 6.2-22 we need volumetric equation-of-state data, that is, information on the interrelationship between P , V , and T . This information may be available as tables of experimental data, or, more frequently, as approximate equations with parameters that have been fitted to experimental data. Hundreds of analytic equations of state have been suggested for the correlation of P V T data.

$\left(P+\frac{a}{\underline{V}^2}\right)(\underline{V}-b)=RT$ or equivalently $P=\frac{RT}{\underline{V}-b}-\frac{a}{\underline{V}^2}$. (Equation 5.1)

with a and b constants, was proposed by J. D. van der Waals in 1873 to describe the volumetric or P V T behavior of both vapors and liquids, work for which he was awarded the Nobel Prize in Physics in 1910. The constants a and b can be determined either by fitting this equation to experimental data or, more commonly, from critical-point data as will be described in Sec. 6.6. Values for the parameters for several gases appear in Table 6.4-1. These parameters were computed from critical-point data as described in Sec. 6.6.

### 5.2.2 Application of Peng-Robinson Equation of State

It must be emphasized that the van der Waals equation of state is not very accurate and has been used here merely for demonstration because of its simplicity. It is never used

for engineering design predictions, though other cubic equations of state are used. To illustrate the use of generalized equations of state, we will consider only the Peng-Robinson equation, which is commonly used to represent hydrocarbons and in-organic gases such as nitrogen, oxygen, and hydrogen sulfide. The generalized form of the Peng-Robinson equation of state is:

$$P = \frac{RT}{\underline{V} - b} - \frac{a(T)}{\underline{V}(\underline{V} + b) + b(\underline{V} - b)}$$

with

$$a(T) = 0.45724 \frac{R^2 T_c^2}{P_c} \alpha(T)$$

$$b = 0.07780 \frac{RT_c}{P_c}$$

$$\sqrt{\alpha} = 1 + \kappa \left(1 - \sqrt{\frac{T}{T_c}}\right)$$

and

$$\kappa = 0.37464 + 1.54226\omega - 0.26992\omega^2. \quad \text{(Equation 5.2)}$$

```
% Solve for V_HP1
syms V_HP1sym
  Tr_HP1 = T_HP1 / Tc_R410a;
  ALPHASqrt1 = 1 + Kappa_R410a * (1 - sqrt(Tr_HP1));
  Alpha_VCC4 = ALPHASqrt1^2;
  aT_HP1 = aTc_R410a * Alpha_VCC4;
  SV_HP1sym = solve(P_HP1 == R*T_HP1 / (V_HP1sym-b_R410a) - ...
                  aT_HP1 / (V_HP1sym*(V_HP1sym+b_R410a) + ...
                  b_R410a*(V_HP1sym-b_R410a)));
  V_HP1 = double(SV_HP1sym);
  V_HP1 = V_HP1(imag(V_HP1)==0);
```

In general, we expect three independent properties to be required to specify state for a binary mixture such as aqueous lithium bromide. However, because the pressure effect is usually small, it is often omitted from property correlations for this mixture.

Numeric values for equation-of-state parameters are commonly obtained in one of two ways. First, parameters can be obtained by fitting the equation to P V T and other data for the fluid of interest; this leads to the most accurate values, but is very tedious. Second, as will be discussed in Sec. 6.7, general relations can be obtained between the equation-of-state parameters and critical-point properties. From these equations, somewhat less accurate parameter values are easily obtained from only critical-point properties.

Each of the equations of state discussed here can be written in the form:

$Z^3 + \alpha Z^2 + \beta Z + \gamma = 0$. (Equation 5.5)

where the parameters can be found in the following table:

| | van der Waals | Redlich-Kwong and Soave | Peng-Robinson |
|---|---|---|---|
| $\alpha$ | $-1-B$ | $-1$ | $-1+B$ |
| $\beta$ | $A$ | $A-B-B^2$ | $A-3B^2-2B$ |
| $\gamma$ | $-AB$ | $-AB$ | $-AB+B^2+B^3$ |

where

$Z = P\underline{V}/RT$

$B = bP/RT$

and

$$A = \begin{cases} aP/(RT)^2 & \text{in the van der Waals, Soave, and Peng-Robinson equations of state} \\ aP/R^2T^{2.5} & \text{in the Redlich-Kwong equation of state} \end{cases}$$

.

where Z = P V /RT is the compressibility factor, and the parameters α, β, and γ for some representative equations of state are given in Table 6.4-3. Consequently, these equations are said to be cubic equations of state. Many such equations have been suggested in the scientific literature. One should remember that all cubic equations of state are approximate; generally, they provide a reasonable description of the P V T behavior in both the vapor and liquid regions for hydrocarbons, and of the vapor region only for many other pure fluids. The Soave–Redlich-Kwong and the Peng-Robinson equations are, at present, the most commonly used cubic equations of state.

## 5.3 Calculation of Enthalpy and Entropy

Enthalpy and entropy of ideal gas can be calculated by the following code.

```
% Enthalpy and Entropy Change from Reference State of Ideal Gas.
H_IG = AAA * (T(l)-T_ref) + BBB * (T(l)^2-T_ref^2)./2 + ...
      CCC * (T(l)^3-T_ref^3)./3 + DDD * (T(l)^4-T_ref^4)./4;    % Ideal Gas
S_IG = AAA * log(T(l)./T_ref) + BBB * (T(l)-T_ref) + ...
      CCC * (T(l)^2-T_ref^2)./2 + DDD * (T(l)^3-T_ref^3)./3;    % Ideal Gas
S_IG = S_IG - R * log(p(m)/p_ref);                          % Ideal Gas
H = DH + H_IG;
S = DS + S_IG;
```

This generalized form of the Peng-Robinson equation of state (or other equations of state) can be used to compute not only the compressibility, but also the departure

functions for the other thermodynamic properties. This is done using Eqs. 6.4-29 and 6.4-30. In particular, to obtain numerical values for the enthalpy or entropy departure for a fluid that obeys the Peng-Robinson equation of state, one uses the following procedure:

```
% Define General Constants and Constants for R123.
R = 8.314472;                % J/(mol*K), Universial Gas Constant
M = 18 / 1000;               % kg / mol , Molar Mass
R_G = 0.0544 * 1000;          % J/(K*kg) , Gas Constant - R123
AAA =  39.49E-3;             % C_p1, heat capacity calculation parameter of R123
BBB = -2.743E-5;              % C_p2, heat capacity calculation parameter of R123
CCC = -0.122E-8;              % C_p3, heat capacity calculation parameter of R123
DDD =  0.572E-11;             % C_p4, heat capacity calculation parameter of R123
T_c = 456.83;                % K  , temperature in Critical Point.
p_c = 3668.0 * 1000;          % Pa , pressure in Critical Point.
OMEGA = 0.281922497036;       % Acentric Factor.
Tboil = 273.15 + 27.85;       % K  , Boiling point at one atmosphere.
T_ref = 273.15;              % K  , temperature in reference state
p_ref = 101.325 * 1000;       % Pa , pressure in reference state
```

```
% Calculate the Parameters in Peng-Robinson Equation of State.
a_Tc = 0.457235529 * (R_G * T_c)^2 ./ p_c;            % Critical Point Restriction
"a(T_c)"
KAPPA = 0.37464 + (1.54226 - 0.26992 * OMEGA) * OMEGA;  % Dependent on OMEGA
T_r = T(l) ./ T_c;                                  % Reduced Temerature
ALPHASqrt = 1 + KAPPA * (1 - sqrt(T_r));
ALPHA = ALPHASqrt^2;                                 % Temperature-dependent para in
PR
a_T = a_Tc * ALPHA;                                  % Temperature-dependent para in
PR
b = 0.077796074 * R_G * T_c ./ p_c;                    % m^3/mol, Critical Point
Restriction
DADT = - a_Tc * KAPPA * ALPHASqrt ./ sqrt(T_c * T(l));  % partial(a) / partial(T)
A = a_T * p(m) ./ ((R_G * T(l))^2);                    % Parameters for Cubic Form
B = b * p(m) ./ (R_G * T(l));                         % Parameters for Cubic Form
```

The procedure is shown as following:

1. Use the critical properties and acentric factor of the fluid to calculate b, κ, and the temperature-independent part of a using equation 5.2.
2. At the temperature of interest, compute numerical values for α and a using equation 5.2.
3. Solve the equation of state, equation 5.1, for V and compute **`Z = P V / (R T)`**. Alternatively, solve for Z directly from the equivalent equation

$$Z^3-(1-B)Z^2+(A-3B^2-2B)Z-(AB-B^2-B^3)=0 \quad \text{(Equation 5.3)}$$

where **B = P b / (R T)** and **A = a P / (R^2 T^2)**.

4. Use the computed value of Z and

$$\frac{da}{dT}=-0.45724\frac{R^2T_c^2}{P_c}\kappa\sqrt{\frac{\alpha}{TT_c}} \quad \text{(Equation 5.4)}$$

to compute [H(T,P)− $H^{IG}$(T,P)] and/or [S(T,P)− $S^{IG}$(T,P)] as desired, using following Equation 5.5 and Equation 5.6.

```
% Solve the Equation of State using Determining Equation.
function [Z_g,Z_l] = ZZroot2(A,B)
c1 = B - 1;
c2 = A - 3 * B^2 - 2 * B;
c3 = B^3 + B^2 - A*B;
q = 2/27 * c1^3 - c1*c2/3 +c3;
r = c2 - c1^2 / 3;
D = q^2 / 4 + r^3 / 27;                          %
OMEGA1 = (-1 + sqrt(3) * 1i) / 2;
OMEGA2 = (-1 - sqrt(3) * 1i) / 2;
Z1 = (-q/2 + sqrt((q/2)^2 + (r/3)^3))^(1/3) + ...
    (-q/2 - sqrt((q/2)^2 + (r/3)^3))^(1/3);
Z2 = OMEGA1 * (-q/2 + sqrt((q/2)^2 + (r/3)^3))^(1/3) + ...
    OMEGA2 * (-q/2 - sqrt((q/2)^2 + (r/3)^3))^(1/3);
Z3 = OMEGA2 * (-q/2 + sqrt((q/2)^2 + (r/3)^3))^(1/3) + ...
    OMEGA1 * (-q/2 - sqrt((q/2)^2 + (r/3)^3))^(1/3);
ZZZ = [Z1 Z2 Z3];                                %
ZZZ = ZZZ(imag(ZZZ)==0);                         %
if D > 0
   Z_g = ZZZ(1);
   Z_l = 0;
else
   Z_g = max(ZZZ);
   Z_l = min(ZZZ);
end
end
```

Enthalpy and entropy changes for the Peng-Robinson equation of state:

$$\underline{H}(T,P)-\underline{H}^{\mathrm{IG}}(T,P)=RT(Z-1)+\frac{T\left(\frac{da}{dT}\right)-a}{2\sqrt{2}b}\ln\left[\frac{Z+(1+\sqrt{2})B}{Z+(1-\sqrt{2})B}\right], \text{(Equation 5.5)}$$

$$\underline{S}(T,P)-\underline{S}^{\mathrm{IG}}(T,P)=R\ln(Z-B)+\frac{\frac{da}{dT}}{2\sqrt{2}b}\ln\left[\frac{Z+(1+\sqrt{2})B}{Z+(1-\sqrt{2})B}\right]. \quad \text{(Equation 5.6)}$$

```
% Departure H and S between Ideal Gas and Real Gas.
function DepartHS = SolveDepartHS(a_T,b,B,Z,DADT,T,p,R,R_G)
for i=1:2,
    ParaFuga1(i) = log((Z(i)+(1+sqrt(2))*B)/(Z(i)+(1-sqrt(2))*B));
    DH(i) = (T * DADT - a_T) * ParaFuga1(i)/b/sqrt(8);
    DH(i) = R * T * (Z(i)-1) + DH(i) * R/R_G;
    %Gas Enthalpy Departure , EQN 4.4-29
    DS(i) = DADT*ParaFuga1(i)/b/sqrt(8);
    DS(i) = R*log((Z(i)-B))+DS(i)*R/R_G;
    %Gas EnT_ropy Departure , EQN 4.4-30
end
DepartHS = [DH DS];
end
```

The enthalpy and entropy departures from ideal gas behavior calculated in this way can be used to solve thermodynamic problems in the same manner as the similar functions obtained from the corresponding-states graphs were used in the previous section.

## 5.4 Vapor Pressure and Liquid Density

The most important saturation property is therefore the vapor pressure, which can be determined experimentally by a number of techniques [20]. Once the saturation line is defined, it is possible to consider the properties of both coexisting phases at saturation, including the density and heat capacity. The density of the vapor at saturation is seldom measured directly owing to the difficulties involved so that it is frequently obtained indirectly. On the other hand, the liquid phase density at saturation is more easily measured. Heat capacity measurements in both liquid and vapor phases are possible [21]. It is noteworthy that in the liquid phase it is possible to define three specific heat capacities, the change in enthalpy with temperature at constant pressure, the change in enthalpy with temperature for the saturated liquid, the energy required to effect a temperature change while maintaining the liquid in a saturated state. The three heat capacities do not generally differ by very much. Estimation methods for saturated densities and heat capacities at saturation are available [22].

```
% Calculate T_4 in ORC_R123 through Equation of Pressure of Pure Saturated Vapor
syms T_4sym
A =  1.656333E3;  B = -2.480583E6; C = 1.792522E1;
D = -8.868380E-2; E =  4.617861E2; F = 1.666667E3;
ST_4sym = solve(log10(P_ORC4/1000) == A + B/T_4sym + ...
          C * log10(T_4sym) + D * T_4sym + ...
```

```
        E * ((F-T_4sym)/T_4sym) * log10(F-T_4sym));
        T_ORC4 = double(ST_4sym);
        T_ORC4 = real(T_ORC4);
```

```
% Calculate v_1 in ORC_R123 through Equation of Density of Pure Saturated Liquid
Af_R123 = 4.643358E2; Bf_R123 =  1.625985E3; Cf_R123 = -1.333543E3;
Df_R123 = 1.986142E3; Ef_R123 = -7.172430E2;
Tr_ORC1 = T_ORC1 / Tc_R123;
D_ORC1 = Af_R123 + Bf_R123 * (1-Tr_ORC1).^(1/3) + ...
        Cf_R123 * (1-Tr_ORC1).^(2/3) + ...
        Df_R123 * (1-Tr_ORC1) + Ef_R123 - (1-Tr_ORC1).^(4/3);
V_ORC1 = 1 / D_ORC1;
```

## 5.5 Temp and Pressure of Binary Saturated Solution

Temp of Binary Saturated Solution can be calculated from Dew point nd solution temperature of lithium bromide solution:

$$t = (a_o + a_1X + a_2X^2 + a_3X^3)t' + (b_o + b_1X + b_2X^2 + b_3X^3)$$

where $a_o = -2.00755$, $a_1 = 0.16976$, $a_2 = -3.13336E-3$, $a_3 = 1.97668E-5$; $b_o = 124.937$, $b_1 = -7.7165$, $b_2 = 0.152286$, $b_3 = -7.9509E-4$

Range: $-20 < t' < 110C$, $5 < t < 180C$, $45\% < X < 70\%$

```
% K, Calculate T_1 of saturated liquid solution through Duhring Equation.
Tw_AC1 = CoolProp.PropsSI('T', 'P', P_AC1, 'Q', 0, 'Water') - 273.15;
a0_alb = -2.00755; a1_alb = 0.16976; a2_alb = -3.13336E-3; a3_alb = 1.97668E-5;
b0_alb = 124.937;  b1_alb = -7.7162; b2_alb = 0.152286;    b3_alb = -7.9509E-4;
T_AC1 = Tw_AC1 * (a0_alb + a1_alb * (y_1*100) + a2_alb * ...
        (y_1*100)^2 + a3_alb * (y_1*100)^3) + b0_alb + ...
        b1_alb * (y_1*100) + b2_alb * (y_1*100)^2 + b3_alb * (y_1*100)^3 + 273.15;
```

Pressure of Binary Saturated Solution:

```
% Pa, Calculate p of saturated liquid solution
D = 6.21147; E = -2886.373; F = -337269.46;
Log(p) = D + E / T + F / T^2;
```

## 5.5 Softwares for Thermal Property

### 5.5.1 REFPROP

REFPROP is an acronym for REFerence fluid PROPerties. This program, developed by the National Institute of Standards and Technology (NIST), calculates the

thermodynamic and transport properties of industrially important fluids and their mixtures. These properties can be displayed in tables and plots through the graphical user interface; they are also accessible through spreadsheets or user-written applications accessing the REFPROP DLL or the FORTRAN property subroutines.

### 5.5.2 CoolProp

The mixture modeling used in CoolProp is based on the work of Kunz et al. [23][24] and Lemmon [25][26][27].

A mixture is composed of a number of components, and for each pair of components, it is necessary to have information for the excess Helmholtz energy term as well as the reducing function. See below for what binary pairs are included in CoolProp.

The numerical methods required for mixtures are far more complicated than those for pure fluids, so the number of flash routines that are currently available are relatively small compared to pure fluids.

The only types of inputs that are allowed for mixtures right now are: Pressure/quality, Temperature/quality, and Temperature/pressure.

# Chapter 6 Case Study & Result

## 6.1 Optimization of MGT

As the main fuel energy converting device, MGT is very important, because the AC_ALB and ORC_R123 can be seen as devices recycling waste heat. So, more attention has been paid to the configuration of MGT by performing a separate optimization. This optimization is relatively in high speed because of less variables. A part of main function code is shown below, which create the first generation, And the result is shown in the following chart.

```
ObjectiveFunction = @simple_fitness;
nvars = 5;                                      % Number of variables
lb = [250*1000; 0.8; 0.8;  700; 1100];               % Lower bound
ub = [650*1000; 0.9; 0.93; 900; 1300];              % Upper bound
ConstraintFunction = @simple_constraint;
rng(1,'twister')                                 % for reproducibility
X0(:,1) = round(rand(1,100)*400*1000) + 250000;
X0(:,2) = round(rand(1,100)*100) + 800;
X0(:,2) = X0(:,2) / 1000;
X0(:,3) = round(rand(1,100)*130) + 800;
X0(:,3) = X0(:,3) / 1000;
X0(:,4) = round(rand(1,100)*200) + 700;
X0(:,5) = round(rand(1,100)*200) + 1100;
```

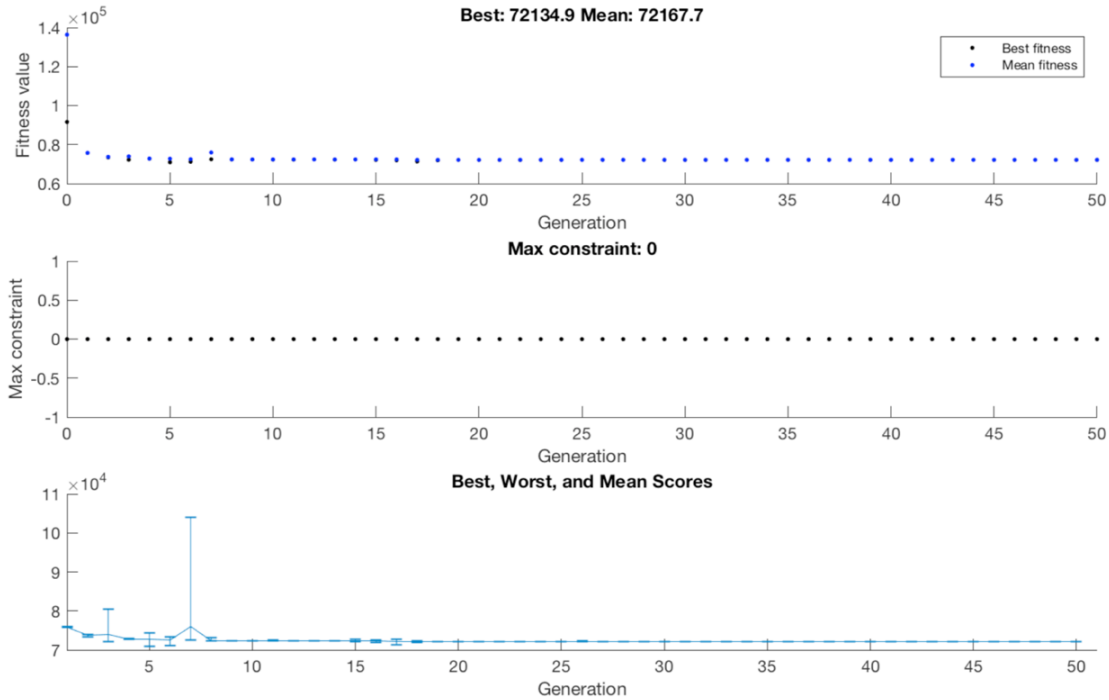


Figure 6.1 Genetic algorithm optimization of micro gas turbine

## 6.2 GEI in Southern China

The following form is formulated to assist creation of initial population.

Northern Area ○ / Southern Area ○

```
Ms = _______; Mcw = _______;

Wp_MGT = 50 kW; T_7 = 550 K; T_wg = 373.15 K;
x(1:5) = [_______, _______, _______, _______, _______];
```

| Constraints | x(1) | x(2) | x(3) | x(4) | x(5) |
|---|---|---|---|---|---|
| lb | | | | | |
| ub | | | | | |

```
MsDV_MGT = _______; MgDV = _______; MaDV = _______; MfDV = _______;
DVm_MGT = _______;
Ms_MGT = MsDV_MGT * DVm_MGT = _______; Mg = MgDV * DVm_MGT = _______;

T_AC11 = T_7; T_AC12 = T_AC11 - (T_AC11 - T_wg) * 0.8; MwDV_AC = 1 kg/s;
x(8:13) = [_______, _______, _______, _______, _______];
DVm_AC = _______;
Mw_AC = MwDV_AC * DVm_AC = _______;

T_ORC19 = T_AC12; T_ORC20 = T_wg; MwDV_ORC = 1 kg/s;
x(14:17) = [_______, _______, _______, _______];
DVm_ORC = _______;
Mw_ORC = MwDV_ORC * DVm_ORC = _______;
```

The frequency of occurrence of failures is declining as time goes by, which means that the unqualified individuals are eliminated, so there is less and less unqualified individuals in the next generation. There is even a time node, passed which there is no unqualified individuals.

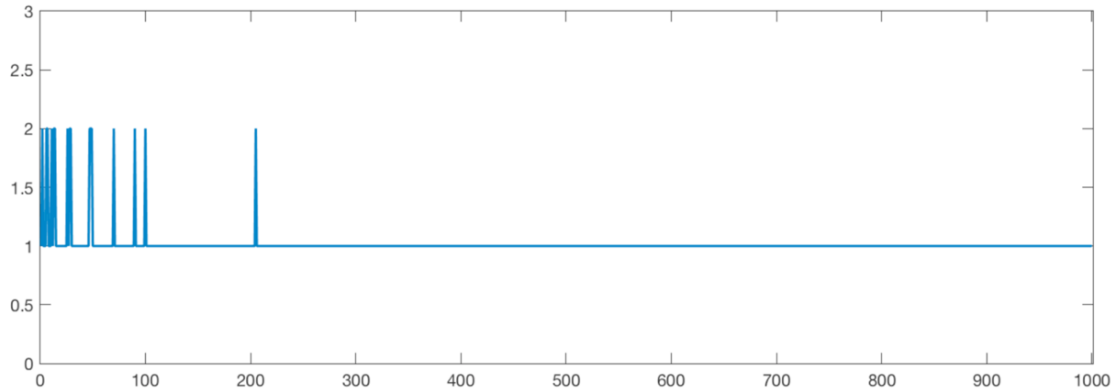


Figure 6.2 Frequency diagram of evaluation failure.

The optimization result has been printed in command window of MATLAB, and the screenshots of the result is shown below.

```
success
success
success
success
success
    3           7329    1.0082e+07    2.864e-05      0
Optimization terminated: average change in the fitness value less than options.FunctionTolerance
 and constraint violation is less than options.ConstraintTolerance.
The number of generations was : 3
The number of function evaluations was : 7329
The best function value found was : 1.0082e+07

>> x

x =

  Columns 1 through 4

          601773.40950842         0.898465846252458         0.923385175368905          903.409030275033

  Columns 5 through 8

         1294.51798951257                      0.03                  25000000          275.146884442368

  Columns 9 through 12

         298.162252405682         0.523679068830945         0.676790890397581          7.59650937500064

  Columns 13 through 16

        0.645155494263045          61.9999848110138          458.144482028373          496799.152328583

  Columns 17 through 20

         311.156417685357          204.975514621883          343.149999997863          275.631037974871

  Column 21

         341.154297247554
```

The optimization result is shown below.

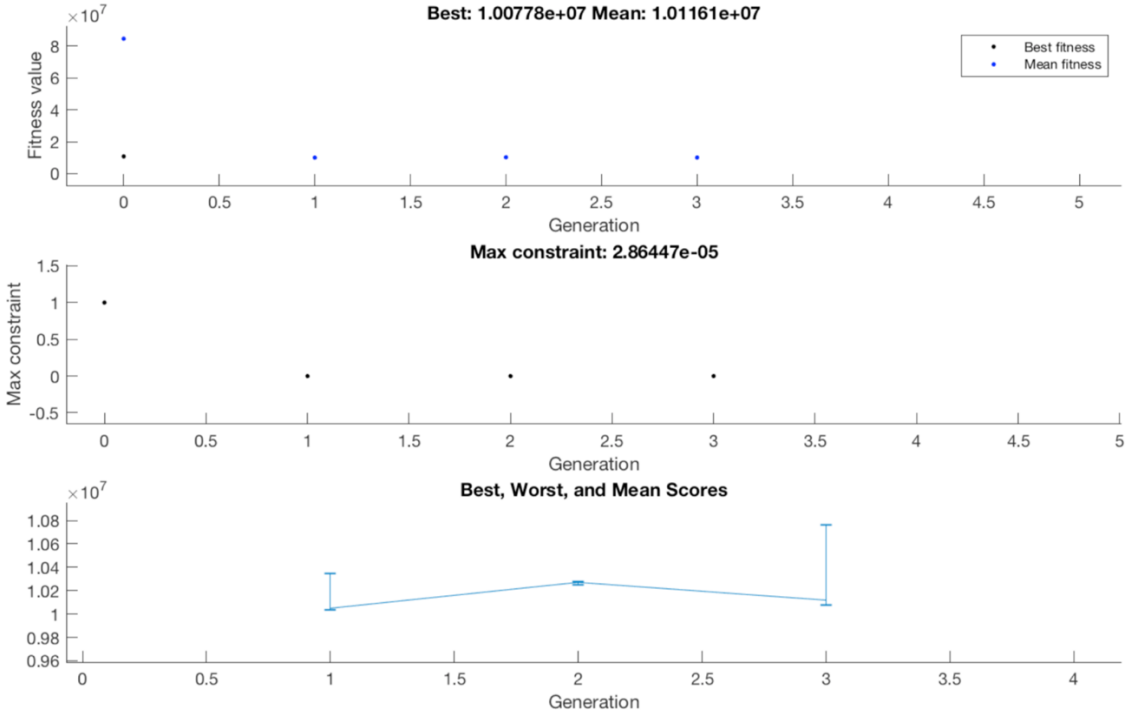


Figure 6.3 Genetic Algorithm Optimization of GEI DER System

# Chapter 7 Conclusion

There are two main tasks in this research, mathematical modeling (integration) and optimization, and the most important part is modeling, which determines the output of the analysis. With three pieces of complicated thermal equipment and many supplementary facilities, modeling is also the toughest task. And there is a trade-off in accuracy of the model. Because if the model is relatively too simple, simulation result will not reflect the real action under various conditions. On the other hand, the complexity can lower the efficiency of optimization.

When programming the model, engineers must follow thermodynamic laws to set energy balance, material balance and flow pressure drop as constraints. State variables and objective functions can only be expressed correctly when engineers base on these principles from various related field like automatic control, statistics, engineering economics, among which principles of multi-energy complementation and cascading utilization are most important two.

As for optimization, because of the application of computer tools like MATLAB optimization toolbox, mixed integer linear programming is easy to start with. In contrast, there is less research based on genetic algorithm, which requires precise representation scheme of problem and appropriate evolution and crossover methods.

When an optimization problem involves only one objective function, it is a single-objective optimization. Most engineering problems require the designer to optimize a number of conflicting objectives. The objectives are in conflict with each other if an improvement in one objective leads to deterioration in another. Multi-objective problems in which there is competition between objectives may have no single, unique optimal solution. So, it's more complicated and practical than single-objective optimization.

Pre-analyses mentioned above is to determine the air-gas ration and heat-power/cold-power ratio. It's assumed that there is a major product between hot steam and cold water. For example, the case study has chosen the green energy island in southern China, which means more cold water must be supplied than hot steam in general. So, the outlet temperature of waste gas of micro gas turbine is set relatively high and cold-electricity ratio is calculated to meet load of cold water in priority. Whole optimization must be carried out after all assisting variables are determined, because these analyses can shorten

the time of optimization enormously.

When constructing mathematical model, the calculation for thermal properties of different working substances and the exergy analysis are two most important operation. Some important interactions between five thermal properties, temperature, pressure, specific volume, enthalpy and entropy, are explored in this project. It's these relationships that make the result of model accurate and practical. Additionally, each component in every device has been analyzed in the form of exergy destruction and efficiency, which indicate the actual thermodynamic performance.

However, some problems cannot be neglected, and they need further attention. Thermo-economics analysis has to be abandoned for lack of actual parameters, which requires more solid engineering economics knowledge and rich related experience. So, the economic factors in fitness are missing. Besides, the calculations for enthalpy and entropy of various working substances need unification, and it's hard to compute temperature based on pressure and entropy. So, some of the calculation in this project is done by calling non-original program.

# Acknowledgements

I would like to express thanks to:

- Prof. Chen Yang, who guide my project, gave suggestions to my future study and dissertation writing;
- Teacher Hong Peng, Jian Bao, Kunyu Zhong and Rui Zhang, without whose advice and help I can't make to finish my study in Chongqing and go to Denmark Technical University;
- Zequn Yu, Zhaokun Zhou, Shang Zhang, Jianlin Zhu, who always help me and accompanying me when I feel frustrated;
- My parents and all elder relatives, who love and support me with no condition;
- Yanan Wang, who should try her best to pursue her dream.

The project would not have been finished without you.

# Reference


**[1]** Kunz, R. Klimeck, W. Wagner, and M. Jaeschke. The GERG-2004 Wide-Range Equation of State for Natural Gases and Other Mixtures. VDI Verlag GmbH, 2007.

**[2]** Kunz and W. Wagner. The GERG-2008 Wide-Range Equation of State for Natural Gases and Other Mixtures: An Expansion of GERG-2004. J. Chem. Eng. Data, 57:3032–3091, 2012. doi:10.1021/je300655b.

**[3]** Eric W. Lemmon, Richard T. Jacobsen, Steven G. Penoncello, and Daniel G. Friend. Thermodynamic Properties of Air and Mixtures of Nitrogen, Argon, and Oxygen from 60 to 2000 K at Pressures to 2000 MPa. J. Phys. Chem. Ref. Data, 29(3):331–385, 2000. doi:10.1063/1.1285884.

**[4]** Eric W. Lemmon and Richard T. Jacobsen. Equations of State for Mixtures of R-32, R-125, R-134a, R-143a, and R-152a. J. Phys. Chem. Ref. Data, 33(2):593–620, 2004. doi:10.1063/1.1649997.

**[5]** E. W. Lemmon and R. T Jacobsen. A Generalized Model for the Thermodynamic Properties of Mixtures. Int. J. Thermophys., 20(3):825–835, 1999. doi:10.1023/A:1022627001338.

**[6]** Integrated energy systems based on cascade utilization of energy

**[7]** Wang C, Nehrir MH. Power management of a stand-alone wind/photovoltaic/fuel cell energy system. IEEE transactions on energy conversion. 2008 Sep;23(3):957-67.

**[8]** Chong EK, Zak SH. An introduction to optimization, edition 4, chapter 14, 273. John Wiley & Sons; 2013 Feb 5.

**[9]** Chow TT, Zhang GQ, Lin Z, Song CL. Global optimization of absorption chiller system by genetic algorithm and neural network. Energy Buildings. 2002;34(1):103-9.

**[10]** Ki-Moon B. Sustainable energy for all. A Vision Statement. New York, United Nations. 2011 Nov.

**[11]** Knopf FC. Modeling, analysis and optimization of process and energy systems. John Wiley & Sons; 2011 Dec 14.

**[12]** Omu A, Choudhary R, Boies A. Distributed energy resource system optimization using mixed integer linear programming. Energy Policy. 2013;61:249-66.

**[13]** Wang C, Nehrir MH. Power management of a stand-alone wind/photovoltaic/fuel cell energy system. IEEE transactions on energy conversion. 2008 Sep;23(3):957-67.

**[14]** Kemp IC. Pinch analysis and process integration: a user guide on process integration for the

efficient use of energy. Elsevier; 2011 Apr 1.

**[15]** Omu A, Choudhary R, Boies A. Distributed energy resource system optimization using mixed integer linear programming. Energy Policy. 2013;61:249-66.

**[16]** Multi-objective Genetic Algorithm Options, MathWorks Company, https://cn.mathworks.com/help/gads/examples/multiobjective-genetic-algorithm-options.html

**[17]** Hawkes, A.D., Leach, M.A., 2009. Modelling high level system design and unit commitment for a microgrid. Applied Energy 86, 1253–1265.

**[18]** Connolly D, Lund H, Mathiesen BV, Leahy M. A review of computer tools for analysing the integration of renewable energy into various energy systems. Appl Energ. 2010;87(4):1059-82.

**[19]** Medrano, M., Brouwer, J., McDonell, V., Mauzey, J., Samuelsen, S., 2008. Integration of distributed generation systems into generic types of commercial buildings in California. Energy and Buildings 40 (4), 537–548.

**[20]** Ruan, Y., Liu, Q., Zhou, W., Firestone, R., Gao, W., Watanabe, T., 2009. Optimal option of distributed generation technologies for various commercial buildings. Applied Energy 86 (9), 1641–2653.

**[21]** Soderman, J., Petterson, F., 2006. Structural and operational optimization of distributed energy systems. Applied Thermal Engineering. 26, 1400–1408.

**[22]** Soderman, J., Petterson, F., 2006. Structural and operational optimization of distributed energy systems. Applied Thermal Engineering. 26, 1400–1408.

**[23]** Dicorato, M., Forte, G., Trovato, M., 2008. Environmental-constrained energy planning using energy-efficiency and distributed-generation facilities. Renewable Energy 33 (6), 1297–1313.

**[24]** Angrisani, G., Rosselli, C., Sasso, M., 2012. Distributed micro-generation systems. Progress in Energy and Combustion Science 38 (4), 502–521.

**[25]** Tester JW, Tester JW. Sustainable energy choosing among options. Cambridge, MA: MIT Press,; 2012.

**[26]** Alanne, K., Saari, A., 2006. Distributed energy generation and sustainable development. Renewable Sustainable Energy Review 10 (6), 539–558.

**[27]** Alarcon-Rodriguez, A., Ault, G., Galloway, S., 2010. Multi-objective planning of distributed energy resources: a review of the state-of-the-art. Renewable and Sustainable Energy Reviews 14, 1353–1366.